ENGINE BLOCK HEAT REJECTION ENHANCEMENT FOR A FOUR CYLINDER CI ENGINE

HAKAN ALTUĞ

JULY 2022

ÇANKAYA UNIVERSITY

GRADUATE SCHOOL OF NATURAL AND APPLIED SCIENCES

DEPARTMENT OF MECHANICAL ENGINEERING

MASTER'S THESIS IN

MECHANICAL ENGINEERING

ENGINE BLOCK HEAT REJECTION ENHANCEMENT FOR A FOUR CYLINDER CI ENGINE

HAKAN ALTUĞ

JULY 2022

ABSTRACT

ENGINE BLOCK HEAT REJECTION ENHANCEMENT FOR A FOUR CYLINDER CI ENGINE

ALTUĞ, Hakan

Master of Science in Mechanical Engineering

Supervisor: Assoc. Prof. Dr. Ekin Özgirgin Yapıcı

JULY 2022, 67 Pages

The study aims to simulate and analyze the thermal behavior of an internal combustion diesel engine and find a optimal solution for heat rejection of the engine block water jacket of a tractor. Tractors are widely used in rough terrains at high temperatures. They produce massive powers, due to such situations, heat rejection rates play an essential role in the engine to stabilize and protect engine life. During the study the temperature behavior of engine block is simulated to eliminate any possible risks of overheating phenomena in terrain. The cylinder block is surrounded by water jacket and the main engine block. After combustion, generated heat causes the temperature increase on the block, which needs to be cooled and stabilized. Coolant mixtures are also widely used on engine systems to stabilize engine temperature. There is a closed circuit between the water jacket, the coolant, the water pump, the pipes and the radiator.

Tractors work at high temperatures under huge power take of loads with low speeds. Due to low speed, they cannot take advantage of passive cooling effects. Because of that, coolant systems should be designed to overcome any possible overheating situation. The main aim of this study is to analyze the temperature distribution of actual engine model, and make geometrical enhancements on outlet water ports and reduce the average temperature of coolant mixture by using special CFD tools.

Firstly, a literature survey is completed. Water jacket optimization of diesel engines, thermal behavior of engine block, computational fluid dynamics used to make such analysis in engine and on agricultural vehicles keywords are used widely. Many articles, case study samples and referred journals have been inspected.

At the first stage of the study, a 3D model of the engine block is prepared and simplified with CFD tools. The water flow rate of the inlet, pressures of the outlet passages, heat flux after combustion, water pump efficiencies are calculated.

For numerical validation, a realistic test bench is used to compare numerical and analytical results with error rates. A four-cylinder engine is mounted on an engine dynamometer. Worst case scenario is performed. The temperature, pressure and velocity specifications are measured for base engine.

In the scope of numerical studies, analyses are done in STAR CCM+. Calculated boundary conditions and simplified geometry has been used. Three different geometry enhancements are designed and analyzed on STAR CCM+. %6.1 heat coolant rejection enhancement is achieved as a result of this study.

Keywords: Diesel Engine, CFD, Water Jacket Cooling.

ÖZ

DÖRT SİLİNDİRLİ BİR DİZEL MOTORDA MOTOR BLOĞUNUN SOĞUTULMASININ İYİLEŞTİRİLMESİ

Hakan ALTUĞ
Makine Mühendisliği Yüksek Lisans

Danışman: Doç. Dr. Ekin ÖZGİRGİN YAPICI
Temmuz 2022, 67 Sayfa

İçten yanmalı dizel motorlar günümüzde otomotiv, tarım, ulaşım, havacılık ve benzeri alanlarda farklı uygulamalarda sıklıkla kullanılmaktadır. Bu motorlar istenilen güç, iş çıktılarına göre farklı silindir ve hacimde kullanılabilirler. Her içten yanmalı motorda olduğu gibi, yanma sonucu açığa çıkan ısı, motor ve motora bağlı tüm ekipmanların ömrünü korumak adına gözlemlenmeli ve kontrol altına alınmalıdır. Günümüzde içten yanma sonucu ortaya çıkan egzoz gazları için homogolasyon çerçevesinde bir çok sistem kulllanılmakta ve açığa çıkan gazların zararı minimize edilmektedir. Bu sistemlere paralel olarak, motorun ömrünü korumak adına soğutma sistemleri özelinde bir çok detaylı çalışma yapılmış ve günümüzde de devam etmektedir.

Bu çalışmanın en temel amacı, motorda yanma sonucu oluşan motor blok sıcaklıklarının, motor su ceketine ve soğutma suyuna olan etkilerini gözlemlemek ve motor bloğu su ceketi çıkış portları üzerinde iyileştirme yaparak soğutma suyu sıcaklıklarında iyileştirme yapmaktır.

Bu hedefler kapsamında bir çok literatür çalışması incelenmiş olup, motor su ceketi geometrilerinde kullanılan numerik modeller, kullanılan bilgisayar destekli analizler incelenmiştir. Bu incelemeler sonucunda bu teze konu olan çalışma için geometri hazırlama ve sonlu akışkanlar elemanları yöntemi ile çözdürme metod kurguları oluşturulmuştur. Kurgulanan çözümleme modelleri ve deneysel çalışmaları karşılaştırmak adına bir motor dinamometresi kullanılarak gerçek bir motor test edilmiştir. Yüksek motor devirleri sonrasında oluşan radyatör su giriş çıkışları ölçülmüştür. Yapılan ölçümlere paralel olarak numerik çalışmalar başlatılmıştır. Bilgisayar ortamında analiz edilen ve test motorunda ölçülen sıcaklık dağılımlarında dört derecelik bir fark görülmüştür. Literatürde yapılan araştırmalar göz önünde bulundurulduğunda bu farkın yapılan varsayımlar çerçevesinde çok beklenir bir düzeyde olduğu kabul edilmiş ve geometri iyileştirmeleri için çalışmalar başlatılmıştır.

Üç farklı motor bloğu tasarımı yapılmış ve bu tasarımlar analiz edilmiştir. Mevcut motor bloğuna göre ısıl çıktılarda %6.1 iyileşme sağlanmıştır.

Anahtar Kelimeler: Dizel Motorlar, Bilgisayar Destekli Akışkanlar Mekaniği, Isı Ceketinin Sogutulması.

ACKNOWLEDGEMENTS

I want to thank Ekin Özgirgin Yapıcı for her support during all study periods. Her experiences in the advisor role, motivated me to understand more and work hard. I enjoyed learning about her motivations and drives to participate more in the success of my academic career.

I also thank Pelin Altuğ for her kind supports for all parameters in my life.

I also thank Mustafa İlker Çetin who managing me well to reach my goals during this study.

TABLE OF CONTENT

LIST OF FIGURES

LIST OF TABLES

LIST OF SYMBOLS

A	: Fluid Section Area [cm^2]
A_{kb}	: Surface Area of Combustion Chamber [cm^2]
A_p	: Piston Face Area of Flat-Faced Piston [cm^2]
AF	: Air-Fuel Ratio [kg_a/kg_f]
B	: Cylinder Bore [cm]
C	: Constant
C_D	: Discharge Coefficient
F	: Force [N]
F_x	: Forces in the x direction [N]
F_Y	: Forces in the y direction [N]
N	: Engine Speed [rpm]
N_c	: Number of cylinders
P	: Pressure [kPa]
Q	: Heat Transfer [kJ]
T	: Temperature [K] [°C]
T_C	: Temperature of Coolant [K] [°C]
T_a	: Temperature of Air [K] [°C]
T_g	: Temperature of Gas [K] [°C]
T_i	: Temperature of Intake [K] [°C]
T_m	: Temperature of Mixture [K] [°C]
T_w	: Temperature of Wall [K] [°C]
V	: Cylinder Volume [L] [cm^3]
V_c	: Clearance Volume [L] [cm^3]
W	: Work [kJ]
a	: Crank offset (crank radius) [cm]
c_p	: Specific Heat at Constant Pressure [kJ/kg-K]
c_v	: Specific Heat at Constant Volume [kJ/kg-K]
h	: Convection Heat Transfer Coefficient [kW/m^2-K]

h_a	: Convection Heat Transfer Coefficient of Air [kW/m^2-K]
k	: Thermal Conductivity [kW/m-K]
m	: Mass[kg]
ρ	: Density[kg/m3]
ω	: Angular Velocity [rpm/s]
μ	: Dynamic Viscosity [kg/m-s]
μ_g	: Dynamic Viscosity of Gas [kg/m-s]
mm	: Millimeter [mm]

ABBREVIATIONS

ICE	: Internal Combustion Engine
SIE	: Spark Ignition Engine
CIE	: Compression Ignition Engine (Diesel Engine)
FEAD	: Front End Accessory Drive
HTC	: Heat Transfer Coefficient
Nu	: Nusselt Number
K	: Kelvin
C	: Celsius
ATB	: Air to Boil
LAT	: Limiting Ambient Temperature

CHAPTER I
INTRODUCTION

1.1 MOTIVATION AND AIM OF THE THESIS STUDY

Internal combustion diesel engines are being used widely especially in heavy industry and agricultural areas. Tractors are mostly used for agricultural applications which operate on rough terrains and at high temperature environments for low-speed operation causing engine faults such overheating. Under these circumstances, cooling systems for these vehicles have a major importance for faultless operation and better efficiencies. [1]

Enhancement for cooling systems of these engines include some geometrical and or systematical designs such as; increasing the heating capacity of the radiator, increasing water flow rate and pump or radiator geometrical improvements.

Forecasting thermal behavior of engine block gives an opportunity to design cooling packages in the beginning of the projects. Making efficient designs eliminates all possible risks of engine overheating issues and predicts engine life as expected.

1.2 FUNDAMENTALS

An internal combustion engine works to convert chemical and thermal energies to mechanical energy during the combustion of fuel. This combustion phenomena causes temperature and pressure increase on pistons, crankshaft, bushings, oiling pins, bearing caps, base block on the engine and other all dynamical components on engine. The diesel engine strokes are intake, compression, combustion and exhaust. In the intake cycle, the mixture is prepared for good combustion. In the compression cycle, the mixture is compressed to increase power efficiency. Burning starts in combustion stage. Cylinder peak temperature and pressures are occurred on this cycle. All engine components must be designed to eliminate any possible faults on field. To do this from design to test all parts are validated by using numerical and analytical methods.

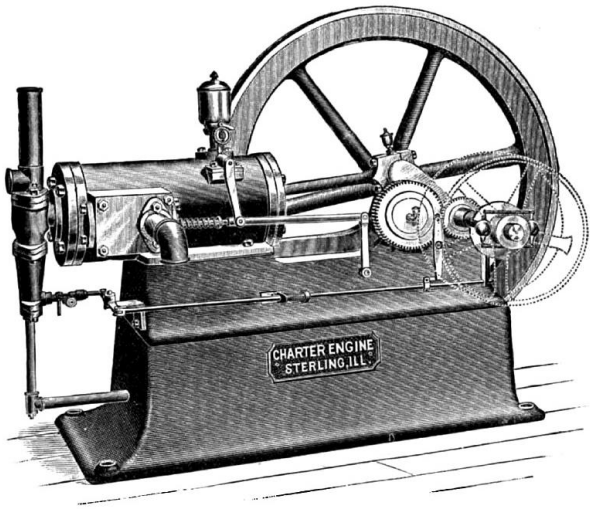

Figure 1.1: The Charter Engine made in 1893 at the Beloit works of Fairbanks, Morse & Company *[2]*

1.2.1 Internal Combustion Engines

Internal combustion engines can be classified in a number of different ways. They are categorized with respect to type of ignitions firstly, compression and spark ignition engines. Second type of classification is engine cycle, four stroke and two stroke. Lastly, they are categorized with respect to location of the valve location, they are categorized with valves in head I head Engine and valves in block, flat head engines. [3]

1.2.1.1 Spark Ignition (SI) Engines

A SI engine starts the combustion process in each cycle use of a spark plug. The spark plug gives a high-voltage electrical discharge between two electrodes which ignites the air-fuel mixture in the combustion chamber surrounding the plug. [3]

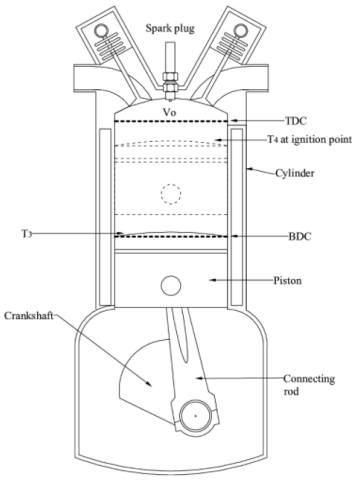

Figure 1.2: Spark Ignition Working Principle with Schematic Representation

1.2.1.2 Compression Ignition (CI) Engines

The combustion prosses in a CI engine starts when the air-fuel mixture self-ignites due to high temperature and pressure in the combustion chamber caused by high compression ratio. [3]

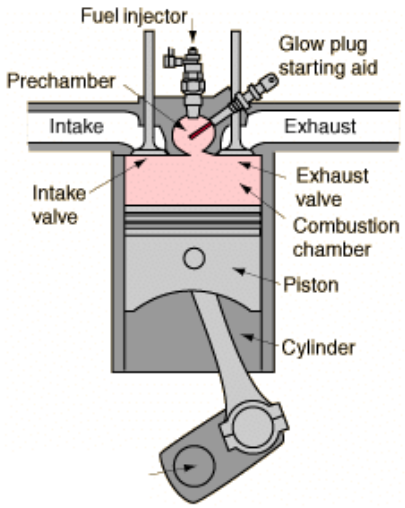

Figure 1.3: Fuel Injector Compression Ignition Diesel Engine Schematic Representation *[4]*

In this study, compression ignition diesel engine is going to be studied. Diesel engines are widely using in agricultural area because diesel engines are more efficient than gasoline engines in terms of fuel consumption.

Four-cylinder diesel engine body is going to be simulated with realistic boundary conditions.

1.2.2 Cooling Systems in Diesel Engines

In Figure 1.4, cooling water cooled engine and cooling systems are shown. Engine, radiator, expansion tank, thermostat, cooling pipes and water pump are the major component of such kind of system. [5]

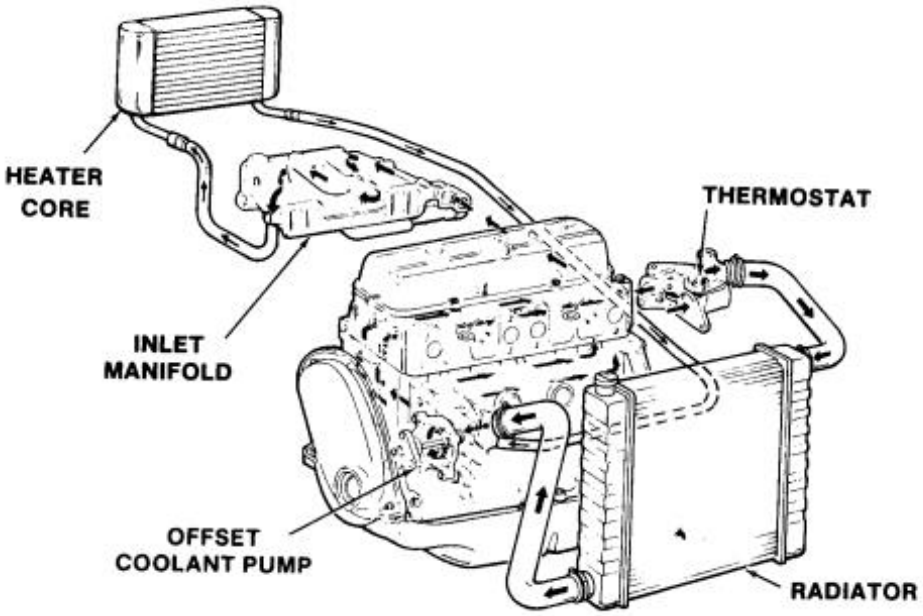

Figure 1.4: Schematic of Cooling System of a Water-Cooled Engine. Reprinted with Permission from SAE Technical Paper 820111-1982, Society of Automotive Engineers, INC. *[6]*

1.2.3 Engine Block

The engine block is the primary parameter of engine systems. All components are mounted on the engine block to resist structural, dynamic and thermal shocks. To do this, base engine blocks are designed to cover all requirements. An engine block also works for transmitting power, reducing the temperature of the components by using a water jacket and lubricating the system to eliminate any fault between parts. [7]

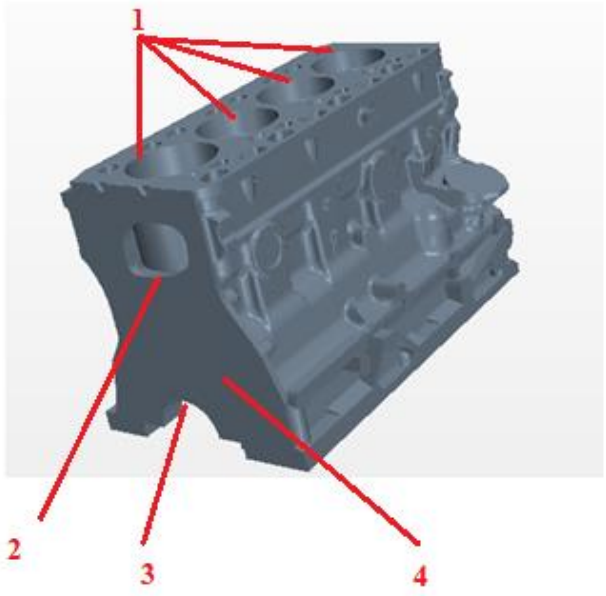

Figure 1.5: Base Engine Three-Dimensional CAD Geometry of Four Cylinder Diesel Engine

As shown in Figure 1.5, there is four-cylinder hole where the combustion is occurs and cylinders moves up-down ward periodically. Number 2 is water intake for cooling system. Number 3 is the crankshaft machined semicircle which is important for assembling of crankshaft, bushings and bearing caps to block. Number 4 is the front face of machined block. All components on front side such as the alternator, the climate compressor, belt tensioners, primary belts, air compressors are mounted on this surface. [8]

On the block there are a variety of passages, internal structures, provisions, machines surfaces, screw threads for assembly accessories.

In diesel engines, listed components are mainly assembled on base engine geometry to run engine. [9]

- Water Pump
- Fuel Dosage or Lifting Pump
- Starter Motor
- Hydraulic Steering Pump
- Fuel Filters
- Oil Cooler
- Connection Rods
- Crankshaft, Camshaft, Gears,

- Pulleys
- Upper Block
- Manifolds
- Oil Sump
- Flywheel
- Pistons
- Glow Plugs
- Injectors
- Bushings

In this study, water jacket of engine block is simulated to analyze thermal behavior of the engine block during combustion to eliminate overheating phenomena.

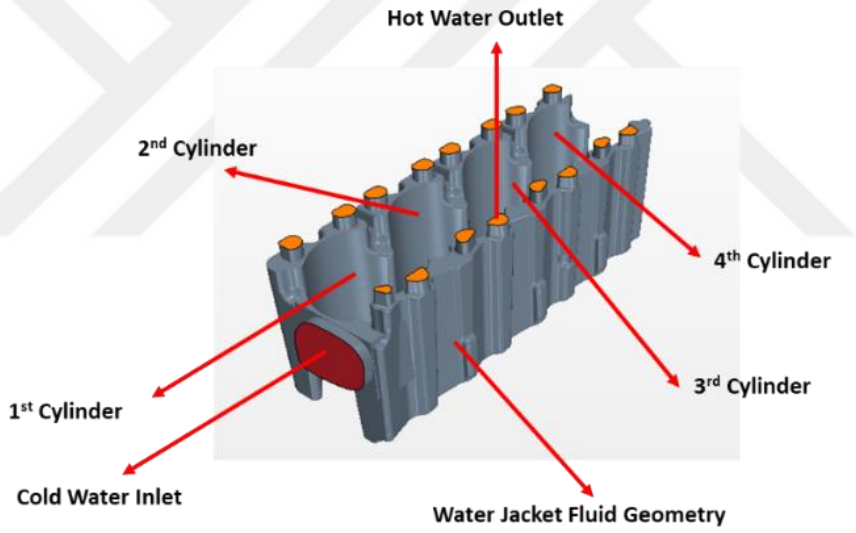

Figure 1.6: Extracted Water Jacket Geometry of Four Cylinder Diesel Engine

In Figure 1.6, extracted water jacket geometry of the four-cylinder diesel engine can be seen. This geometry is called "water jacket geometry" which is the fluid geometry to be simulated with CFD tools.

Red area is cold water inlet passage where pumped water from radiator with low temperature enters. Orange passages are hot water outlets. After combustion, heat is generated inside the engine block, causing temperature increase of both the block walls and water. Water is pumped from block by help of the water pump from orange passages.

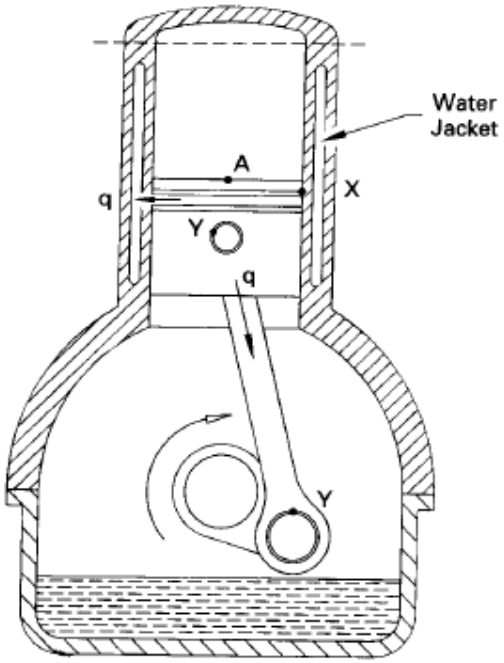

Figure 1.7: Cooling of Piston. The face of piston (A) is one of the hotter surfaces in a combustion chamber *[10]*

Water jacket geometry is designed to cover the outside surface of each cylinder to cool the cylinder walls and to enhance the temperature distribution of the water jacket. This study aims to simulate temperature and pressure distribution among the water jacket and find an optimal design for hot water passages to reduce the total averaged outlet temperature.

1.2.4 Water Pump

In previous sections, base engine block geometry, water jacket of inlet details and cooling system details are presented.

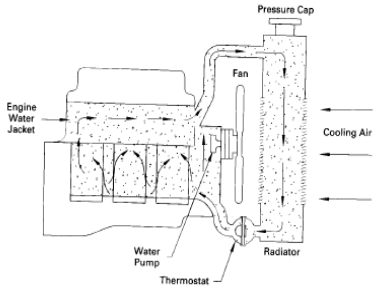

Figure 1.8: Radiator of Liquid-Cooled Engine Used to Remove Heat from The Coolant Loop of the Engine *[11]*

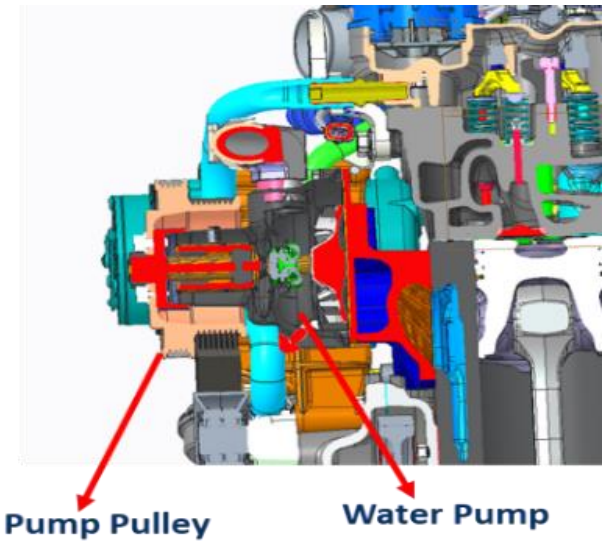

Figure 1.9: Section View of Water Pump

Most systems are of the forced circulation type, which use and engine belt driven water pump, as illustrated in Figure 1.8 and 1.9. In this master of thesis, water pump is assumed as driven by crank pulley and water flow rate changes with the engine main speed. In Figure 1.8 shows assembly details of water pump, there is a tandem mounting between pump pulley which directly driven by crank pulley with a speed ratio, turns water pump impeller and flow rate is generated.

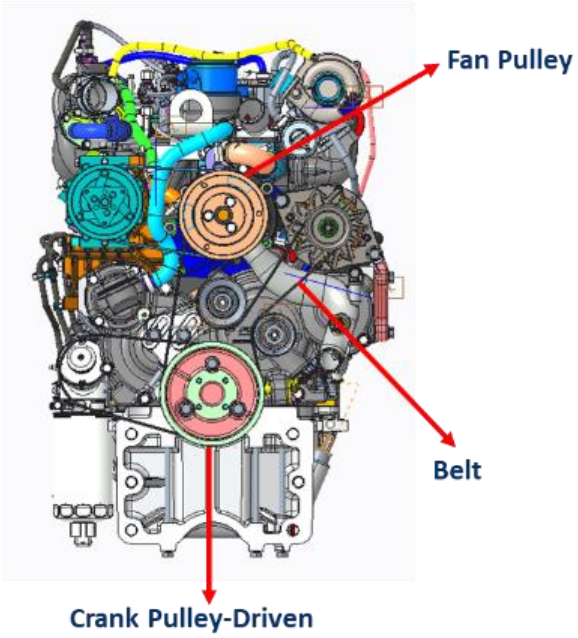

Figure 1.10: Water Pump Mounting Details

In Figure 1.10, water pump mounting details are shown, there is a belt between crank pulley-driver and fan pulley-driven.

1.3 AIM OF THESIS

As the scope of the thesis, performance enhancement methods are investigated for a 4-cylinder diesel engine by design and geometrical or systematical modification of cooling systems for these engines. For this purpose, firstly an analysis of thermal behavior of actual system is done on the engine block 3D geometry and fluid area. Simulations are done by using computational fluid dynamics analysis program to solve temperature distribution of engine block. Secondly, making an optimization of engine block geometry with at least three different cases and reduce the average temperature of outlet ports.

1.4 METHODOLOGY OF THESIS

First step is preparation of CAD model for CFD study seen in Figure 1-5 of the realistic engine block. There are a lot of ports, curvatures and sharp casted geometries on block which cause the analysis to be more difficult and increase analysis time. To make more accurate solutions with reduced solving time ad simplified mesh, inside geometry is simplified.

Secondly, to make realistic CFD analysis, boundary conditions are constituted. Main parameters are water flow rate, cylinder wall temperatures, heat flux, firing orders, Nusselt number, Reynolds number, mass fuel rate, air flow rate and other engine specifications. In calculations sections, all calculated parameters are shown with their formulations.

Next, turbulence modeling is identified. In literature review sections regarding similar studies are presented, steady, k-epsilon turbulence model solving methodology is implemented for the current study.

Next, verification of CFD model with actual engine on test bench is done. Measuring engine inlet and outlet temperatures and pressures with changing speed and comparing the results with the simulation, CFD models are validated.

After verification is completed, geometrical and systematical modifications are done on the engine block, each optimized geometries are run and results are compared with the base engine simulation to see differences between actual geometry and proposed geometry in terms of reduced temperature distribution of outlet ports.

1.4 LITERATURE REVIEW

In the literature there are numerous studies conducted by institutions or academicians to predict thermal behavior of engines. Below most important ones are summarized.

1.4.1 Literature Review 1

Zhang Ping, OuYang Guangyao studied about the flow fluid in cooling water jacket of diesel engine. They solved newton's second law of motion equations in CFD solvers. Also, they solved 6 Cylinder V type diesel engines which the parameters are listed below: [12]

Table 1.1: Three Dimension Model of Cooling Water Jacket *[12]*

Values and Setting	Parameters	Values and Setting	Parameters
Cylinder Bore(mm)	128	Rating Output Power(kW)	186
Stroke(mm)	140	Type of Combustion Chamber	DI

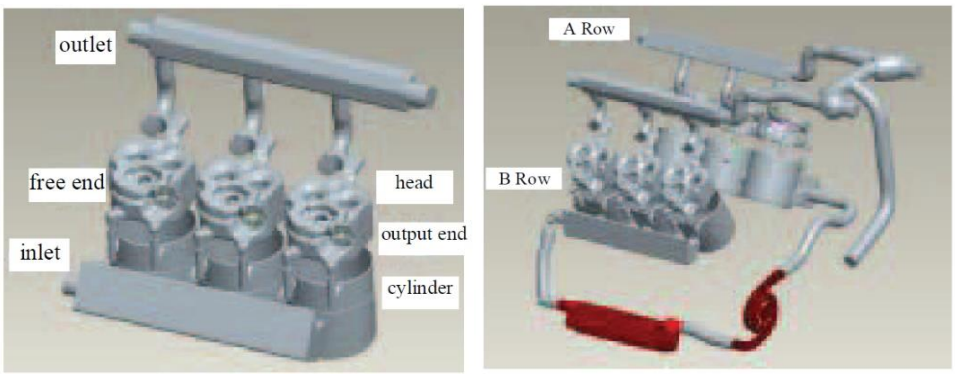

Figure 1.11: Extracted Cooling Water Jacket of Diesel Engine

In Figure 1.11 cooling water jacket is presented. Zhang ping solved only one row of engine block to reduce solving time. They used AVL Fire CFD program during study. They used boundary conditions for inlet and outlet ports, wall functions and turbulence models as tabulated in below in Table 1.2. [12].

Table 1.2: Boundary Conditions and Setting Values *[12]*

Values and Settings	Parameters		
	Mass Flow(kg/s)	Fixed Temperature(K)	Static Pressure(bar)
Inlet Port	2.5	345	
Outlet Port	-		1.02
Wall Function	Standard Wall Function		
Turbulence Model	K-Zeta-F Model		

In Figure 1.12, temperature distributions of water jacket is shown. They calculated the mean heat transfer coefficient as 11582 W/m^2K and the flow velocity 1.16 m/s.

They stated and prove that, if flow resistant force in coolant water is greater, flow pressure is also greater. If losses are tending to decrease, cooling capacity is not enough. The see also 32.6 kPa pressure loss which shows the cooling capacity is well. [12]

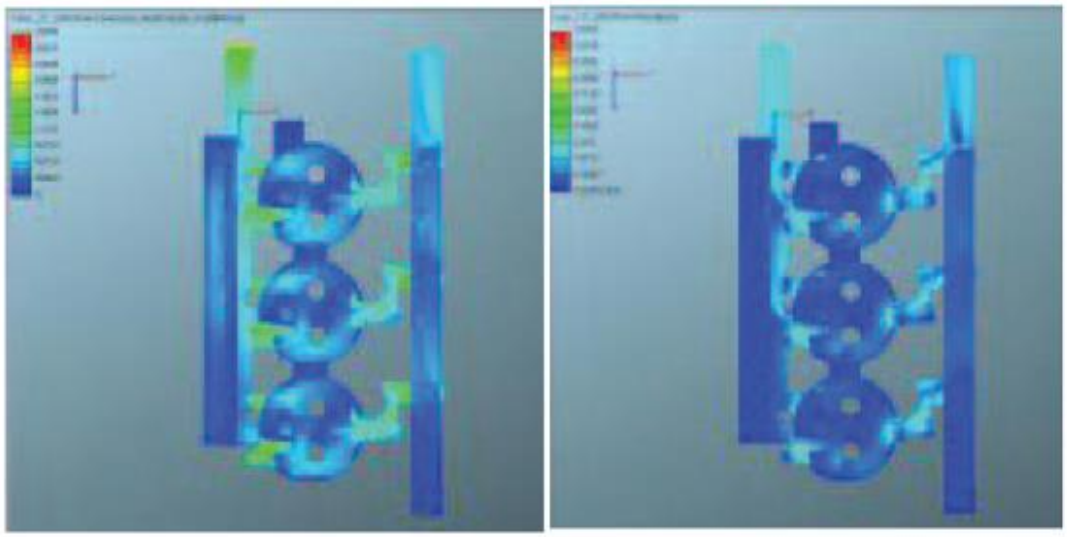

Figure 1.12: Heat Transfer Coefficient Distribution of Cylinder Heat Jacket

1.4.2 Literature Review 2

Yan Zhang studied about flow are and internal flow status of the water jacket. He also studied to analyze pressure loss on the cooling system. They optimized schemes and top face of block to see behaviors. They found that place a baffle at inlet is found to be the best one. [13]

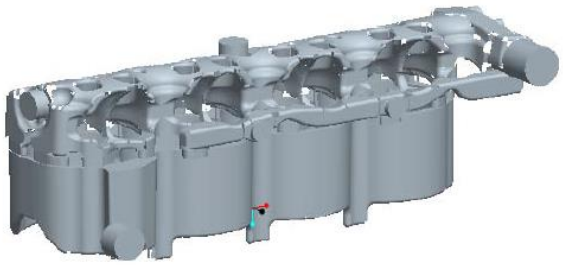

Figure 1.13: 3D Model of Water Jacket *[13]*

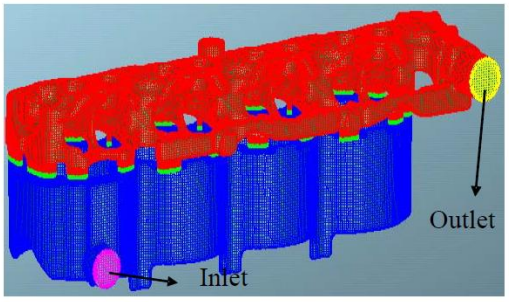

Figure 1.14: Volume Grid Meshed Geometry of Water Jacket *[13]*

In Figure 1.14, cad model is shown. In Figure 1.15, meshed geometry is shown. Grid number is 1,600,000. [13] In Table 1:3, coolant mixture properties are shown.

Table 1.3: The Physical Parameters of Coolant *[13]*

Physical Parameters	Value
Specific Heat Capacity, cp	3302.6 J/(kg.K)
Density,ρ	1000.6 kg/m^3
Kinematic Viscosity, μ	0.000667 kg/m.s
Thermal Conductivity, K	0.4018563 W/(m.K)

The flow of coolant in cylinder and cylinder head is steady state as the engine is working in certain condition. The initial pressure of the whole system is 201325 Pa, the inlet temperature is 373K, the initial value of turbulence kinetic energy is 0.28 m^2/s^2. [13]

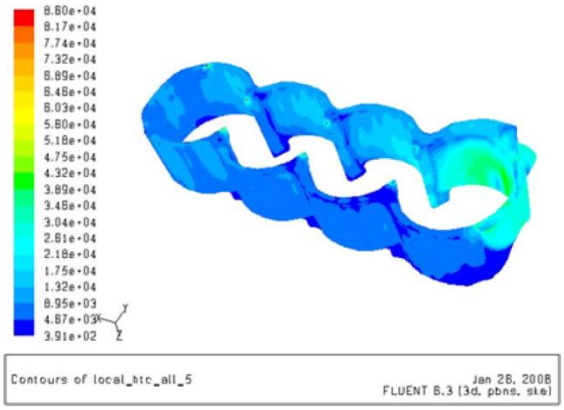

Figure 1.15: Heat Transfer Coefficient Distribution of Water Jacket

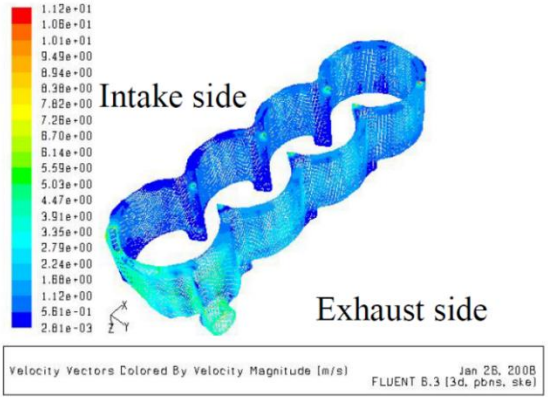

Figure 1.16: Velocity Magnitude [m/s]

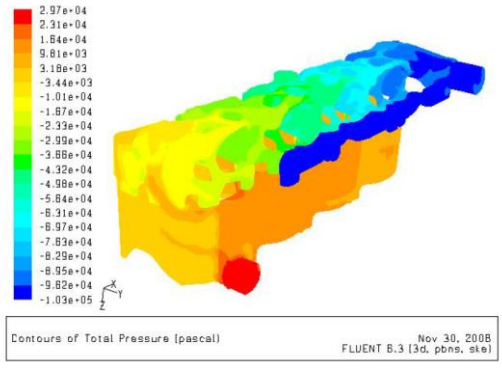

Figure 1.17: Pressure Distribution of Water Jacket

They stated that adding holes on exhaust side using clear sand holes directly effects on water jacket cooling affect also decreased total pressure loss by 16-19 kPa.

1.4.3 Literature Review 3

Bai Lufeng studied on three-dimensional model of HPD diesel engine cooling system water jacket and cylinder head, using AVL software. He simulated temperature of cylinder head was obtained under the condition of rated speed and power. The simulation results showed that there occurred thermal stress and crack on structure [14]. The boundary conditions for water jacket are shown in below tables.

Table 1.4: Properties of Cylinder Head *[14]*

Values and Settings	Parameters		
	Specific Heat (J/(kg*K))	Thermal Conductivity (W/(m*K))	Reference Density (kg/m3)
HT300CuCr	532	58	7000

Table 1.5: Boundary Conditions for Cylinder Head Surfaces *[14]*

Values and Settings	Parameters	
	Fixed Temperature(K)	Heat Transfer Coefficient W/(m2*K)
Outer surfaces	323.15	20
Wall on inlet passage	350.15	400
Wall on outlet passage	823.15	350
Bottom surface	1123.15	571
Adiabatic surface	The quantity of heat flow is zero	
Interface wall	mapping from the simulating calculation on water jacket	

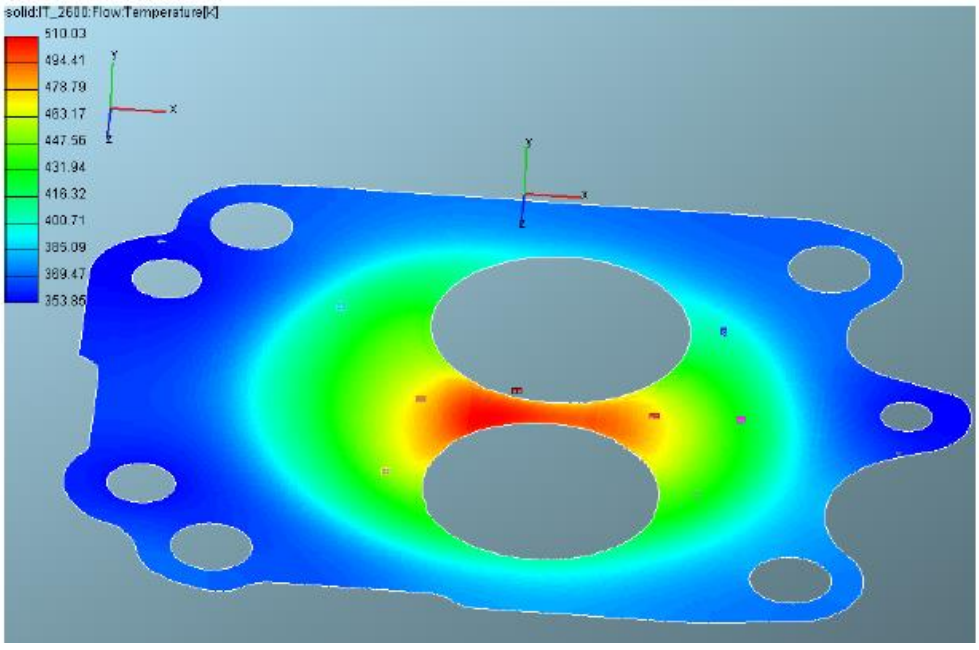

Figure 1.18: Temperature Distribution of Cylinder Block

Highest temperature occurred on cylinder neck as 251°C. They also measure simulated results and they found %2.5 error between values. [14]

1.4.4 Literature Review 4

Gavali and Marathe studied on water jacket cores and they modeled geometry in Pro-Engineer. During the studies they used turbulence k-epsilon turbulence model and they simulated temperature distribution of flow and hot spots in engine block [15].

They studied parallelly two different case study, they did optimization of water transfer hole sizes on barrel and analysis of optimized of barrel, cylinder head and gasket assembly. They used 1,520,000 cells during their CFD analysis. They used 0.47 kg/s mass flow rate, 580°K temperature as boundary condition.

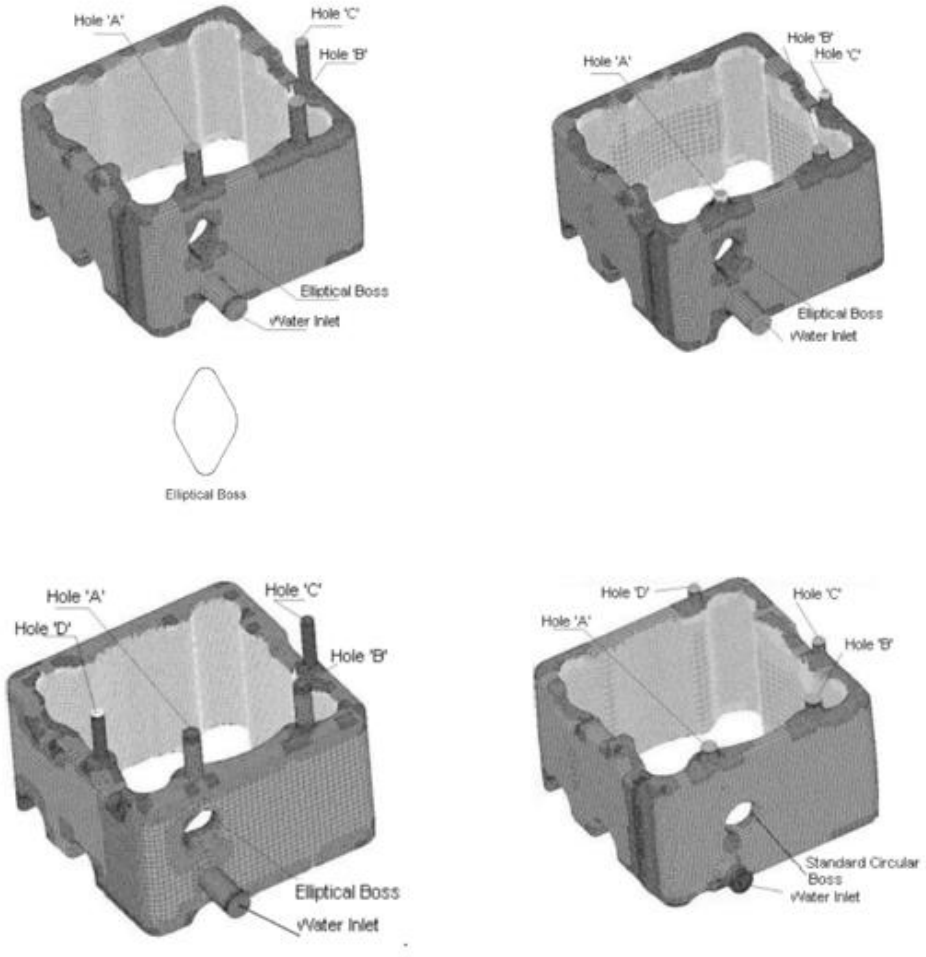

Figure 1.19: Details of Iteration During Simulations [15]

Figure 1.20, shows iterations of added holes one by one. Studies started with three holes and one elliptical boss, but in the end of study they added one extra hole and changed the geometry of water inlet to see heat transfer behavior. [15]

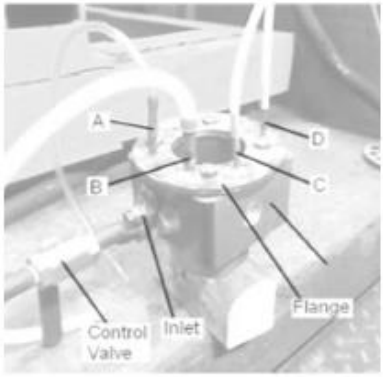

Hole	Velocity (m/s) (Water flow 0.47 kg/s)		% Error
	CFD	EXPERIMENTAL	
A	6.5	5.4	17
B	3	3.5	14
C	6	5.7	5
D	6	5.4	10

Figure 1.20: Experimental Validation and Differences between Computational Data [15]

Results shows that CFD analysis has saved time and cost involved during development of an engine at design stage itself by reducing experimental optimization work. Optimization of water transfer holes, helped to improve cooling of engine, hence increasing of engine components. [15]

1.4.5 Literature Review 5

Wang Zhaowen, Deng Peng have been studied to simulate cooling system of water jacket and cylinder block of engine. They used AVL Fire software and grid model of cooling system water jacket. They calculated temperature of the cylinder head was obtained under the condition of rated speed and power. They stated that thermal stresses and cracks possibilities can be eliminated if geometrical optimization is made on block. [16]

In Figure 1.21, cooling system three-dimensional water model is shown. The volume is extracted from the total body. Outlet and inlet ports are used main boundary condition geometry for water inter and outlet.

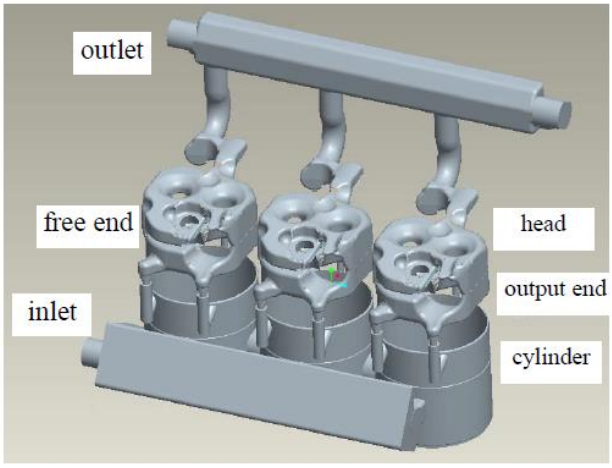

Figure 1.21: Cooling System of Water Model [16]

1.4.6 Literature Review 6

Amit V Paratwar and Hulmar have been studied to predict the temperature of the cylinder head on a six-cylinder v-type diesel engine. They also made a test bench activity to compare with experimental results. [16]

In Table 1.6, the initial conditions for CFD analysis are shown. They have used different temperatures and heat transfer coefficients for each section of the block. [17]

Table 1.6: Initial Conditions for CFD Analysis

Parts	Temperature[K]	Heat Transfer Coefficient[W/m^{2}K]
Deck Face	1200	625
Parts	Temperature[K]	Heat Transfer Coefficient[W/m^{2}K]
Exhaust Port	1000	580
Inlet Port	313	100
Exhaust Valve Guide	313	160
Inlet Valve Guide	313	100
Exhaust Valve Seat	1100	600
Inlet Valve Seat	313	600
Solid Heat	313	100

All CFD simulations were carried out using, the coolant mixture of water and glycol at a constant inlet temperature 373K.

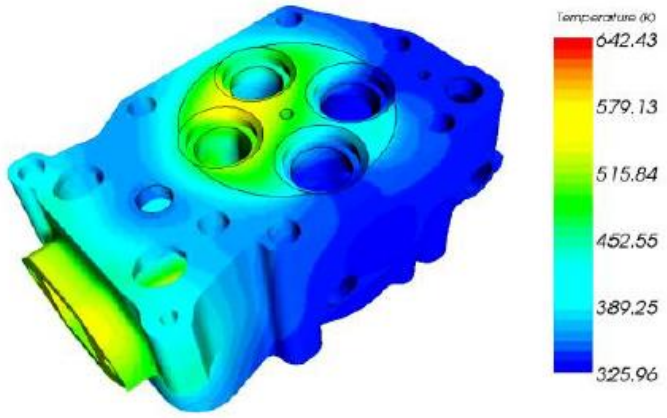

Figure 1.22: Contour of Temperature Distribution of Actual Model

In Figure 1.22, the temperature distribution of actual geometry is shown. They modified their geometries and solved them again in Star CCM. Exhaust port sections are compared in Figure 1.23. %2 temperature enhancement is achieved.

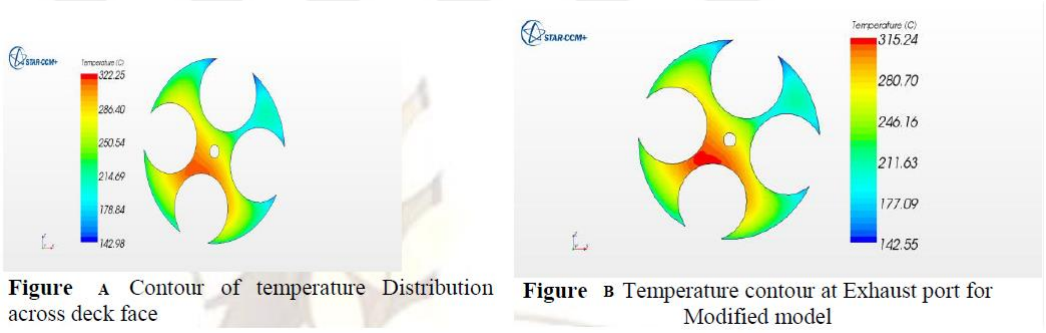

Figure A Contour of temperature Distribution across deck face

Figure B Temperature contour at Exhaust port for Modified model

Figure 1.23: Temperature Contours at Exhaust Port of Actual Geometry (Left) and Modified Geometry (Right)

CHAPTER II
MATHEMATICAL MODELLING

2.1 INTRODUCTION

As it is mentioned in previous section, to observe thermal behavior of water jacket, analysis should be done under the light of mathematical modelling which is given in this section.

2.2 CONTINUITY, NAVIER STOKES AND ENERGY EQUATIONS

Star CCM+ CFD solver based on following continuity and momentum equations based on Newton's Second Law [18]. In each coordinate, Reynolds averaged the Navier-Stokes equations given as below for turbulent flow. [19]

The derivation of the continuity equation is based on the law of conservation of mass, which is derived considering the previously mentioned assumptions. [20]

$$\frac{\partial \bar{u}}{\partial x} + \frac{\partial \bar{v}}{\partial y} + \frac{\partial \bar{w}}{\partial z} = 0 \tag{2.1}$$

Knowing that $\bar{u}$, $\bar{v}$ and $\bar{w}$ are the time average velocity components in the *x*, *y* and *z* directions, respectively.

$$\rho\left(\bar{u}\frac{\partial \bar{u}}{\partial x} + \bar{v}\frac{\partial \bar{u}}{\partial y} + \bar{w}\frac{\partial \bar{u}}{\partial z}\right) = -\frac{\partial p}{\partial x} + \mu\left(\frac{\partial^2 \bar{u}}{\partial x^2} + \frac{\partial^2 \bar{u}}{\partial y^2} + \frac{\partial^2 \bar{u}}{\partial z^2}\right) - \left(\frac{\partial \overline{u'^2}}{\partial x} + \frac{\partial \overline{u'v'}}{\partial y} + \frac{\partial \overline{u'w'}}{\partial z}\right) \tag{2.2}$$

$$\rho\left(\bar{u}\frac{\partial \bar{v}}{\partial x} + \bar{v}\frac{\partial \bar{v}}{\partial y} + \bar{w}\frac{\partial \bar{v}}{\partial z}\right) = -\frac{\partial p}{\partial y} + \mu\left(\frac{\partial^2 \bar{v}}{\partial x^2} + \frac{\partial^2 \bar{v}}{\partial y^2} + \frac{\partial^2 \bar{v}}{\partial z^2}\right) - \left(\frac{\partial \overline{v'u'}}{\partial x} + \frac{\partial \overline{v'^2}}{\partial y} + \frac{\partial \overline{v'w'}}{\partial z}\right) \tag{2.3}$$

$$\rho\left(\bar{u}\frac{\partial \bar{w}}{\partial x} + \bar{v}\frac{\partial \bar{w}}{\partial y} + \bar{w}\frac{\partial \bar{w}}{\partial z}\right) = -\frac{\partial p}{\partial z} + \mu\left(\frac{\partial^2 \bar{w}}{\partial x^2} + \frac{\partial^2 \bar{w}}{\partial y^2} + \frac{\partial^2 \bar{w}}{\partial z^2}\right) - \left(\frac{\partial \overline{w'u'}}{\partial x} + \frac{\partial \overline{w'v'}}{\partial y} + \frac{\partial \overline{w'^2}}{\partial z}\right) \tag{2.4}$$

General heat conduction equation for rectangular coordinates is listed below in Eq. 2.5. [19]

$$\frac{\partial}{\partial x}\left(k\frac{\partial T}{\partial x}\right)+\frac{\partial}{\partial y}\left(k\frac{\partial T}{\partial y}\right)+\frac{\partial}{\partial x}\left(k\frac{\partial T}{\partial z}\right)+\dot{e_g}=\rho c\frac{\partial T}{\partial t} \quad (2.5)$$

2.3 STANDARD k-ε TURBULENCE MODEL

The k-ε turbulence model is the most used computational fluid dynamics turbulence model in CFD applications. Model is based on two equations which give a general solution for transport equations. This turbulence model is based on mean and turbulent kinetic energy [21]. In Eq. 2.5 and Eq. 2.6, mean kinetic and turbulent energy equations are shown respectively.

$$K = \frac{1}{2}\left(U^2+V^2+W^2\right) \quad (2.6)$$

$$k = \frac{1}{2}\left(\overline{u'^2}+\overline{v'^2}+\overline{w'^2}\right) \quad (2.7)$$

$$k(t) = K + k \quad (2.8)$$

If k and ε are known, the turbulent viscosity model can be calculated by using Eq. 2.8. ν_t is turbulent viscosity, ϑ is velocity scale and ℓ is length scale.

$$\nu_t \propto \vartheta\,\ell \propto k^{1/2}\frac{k^{3/2}}{\varepsilon} = \frac{k^2}{\varepsilon} \quad (2.9)$$

The turbulent kinetic energy k and its dissipation rate ε are found from the following transport equations [22]:

$$\frac{\partial}{\partial t}(\rho k)+\frac{\partial}{\partial x_i}(\rho k u_i)=\frac{\partial}{\partial x_j}\left[\left(\mu+\frac{\mu_t}{\sigma_k}\right)\frac{\partial k}{\partial x_j}\right]+G_k+G_b-\rho\varepsilon-Y_M+S_K \quad (2.10)$$

$$\frac{\partial}{\partial t}(\rho\varepsilon)+\frac{\partial}{\partial x_i}(\rho\varepsilon u_i)=\frac{\partial}{\partial x_j}\left[\left(\mu+\frac{\mu_t}{\sigma_\varepsilon}\right)\frac{\partial \varepsilon}{\partial x_j}\right]+G_{1\varepsilon}\frac{\varepsilon}{k}(G_k+C_{3\varepsilon}G_b)-(C_{2\varepsilon}\,\rho\,\frac{\varepsilon^2}{k})+S_\varepsilon \quad (2.11)$$

The steady state k- ε equations that describe the problem can be calculated as follows,

$$\frac{\partial(\mathrm{uk})}{\partial \mathrm{z}}+\frac{1}{\mathrm{r}}\frac{\partial(\mathrm{rvk})}{\partial \mathrm{r}}=\frac{1}{\rho}\frac{\partial}{\partial \mathrm{z}}\left[(\mu+\frac{\mu_t}{\sigma_k})\frac{\partial \mathrm{k}}{\partial \mathrm{z}}\right]+\frac{1}{\rho \mathrm{r}}\frac{\partial}{\partial \mathrm{r}}\left[(\mu+\frac{\mu_t}{\sigma_k})\mathrm{r}\frac{\partial \mathrm{k}}{\partial \mathrm{r}}\right]+\mathrm{G_k}-\varepsilon \quad (2.12)$$

$$\frac{\partial(\mathrm{u}\varepsilon)}{\partial \mathrm{z}}+\frac{1}{\mathrm{r}}\frac{\partial(\mathrm{rv}\varepsilon)}{\partial \mathrm{r}}=\frac{1}{\rho}\frac{\partial}{\partial \mathrm{z}}\left[(\mu+\frac{\mu_t}{\sigma_\varepsilon})\frac{\partial \varepsilon}{\partial \mathrm{z}}\right]+\frac{1}{\rho \mathrm{r}}\frac{\partial}{\partial \mathrm{r}}\left[(\mu+\frac{\mu_t}{\sigma_\varepsilon})\mathrm{r}\frac{\partial \varepsilon}{\partial \mathrm{r}}\right]+\frac{\varepsilon}{\mathrm{k}}(\mathrm{C_1G_k}-\mathrm{C_2}\varepsilon) \quad (2.13)$$

where G_κ represents the generation of turbulence kinetic energy due to the mean velocity gradients defined as:

$$\mathrm{G_k}=-\mu_t\left(2\left(\left(\frac{\partial \mathrm{u}}{\partial \mathrm{z}}\right)^2+\left(\frac{\partial \mathrm{v}}{\partial \mathrm{r}}\right)^2+\left(\frac{\mathrm{v}}{\mathrm{r}}\right)^2\right)+\left(\frac{\partial \mathrm{u}}{\partial \mathrm{r}}+\frac{\partial \mathrm{v}}{\partial \mathrm{z}}\right)^2\right) \quad (2.14)$$

where σk and σε is the turbulent Prandtl numbers for k and ε respectively, c1 and c2 are two constants for the turbulent model [23].

The constants, C_1 = 1.44, C_2=1.92, σ_k=1.0, σ_ε=1.3 and C_μ=0.09

And $\mu_t=\frac{\mathrm{C_\mu}\rho\,\mathrm{k}^2}{\varepsilon}$. (2.15)

2.4 OTHER EQUATIONS

V_h is engine volume, used for calculation of cylinder diameter [mm],

$$V_h=\frac{\pi}{4}d^2h \quad (2.15)$$

Piston crown area, m^2 can be calculated as,

$$A_p=\frac{\pi}{4}d^2 \quad (2.16)$$

To calculate pump properties, below equations can be used, P is Pump Power[Kw], g is gravitational constant $\left[\frac{m}{s^2}\right]$, ρ is density of fluid $[\frac{kg}{m^2}]$, Q is flow rate $[\frac{m^3}{s}]$,

$$\mathrm{P}=\frac{\rho g H Q}{\mu} \quad (2.22)$$

P is Pressure [bar], g is gravitational constant $\left[\frac{m}{s^2}\right]$, ρ is density of fluid $[\frac{kg}{m^2}]$, Q is flow rate $[\frac{m^3}{s}]$

$$P=\rho g H$$

(2.23)

H is pump head[m], g is gravitational constant $\left[\frac{m}{s^2}\right]$, Q is flow rate $[\frac{m^3}{s}]$

$$H = \frac{P}{\rho g Q} \tag{2.24}$$

Speed Ratio Balance for pulleys, where R[mm] is the pulley diameter, N [rpm] is pulley speed.

$$N_1 R_1 = N_2 R_2 \tag{2.25}$$

CHAPTER III
PHYSICAL MODEL FOR CFD SIMULATIONS AND GEOMETRICAL SPECIFICATIONS

3.1 BASE ENGINE BLOCK PREPARATION

As mentioned in previous sections, every diesel engine has a base grey iron casted block of a complex geometry which consists of engine cylinder holes for combustion and produces work to crankshaft. Cooling system consists of a water jacket for coolant water, for lubrication of bearings, caps, gear trains lubrication system is directly mounted on bottom side of block. This geometry is called main component of engine which all components are mounted on it.

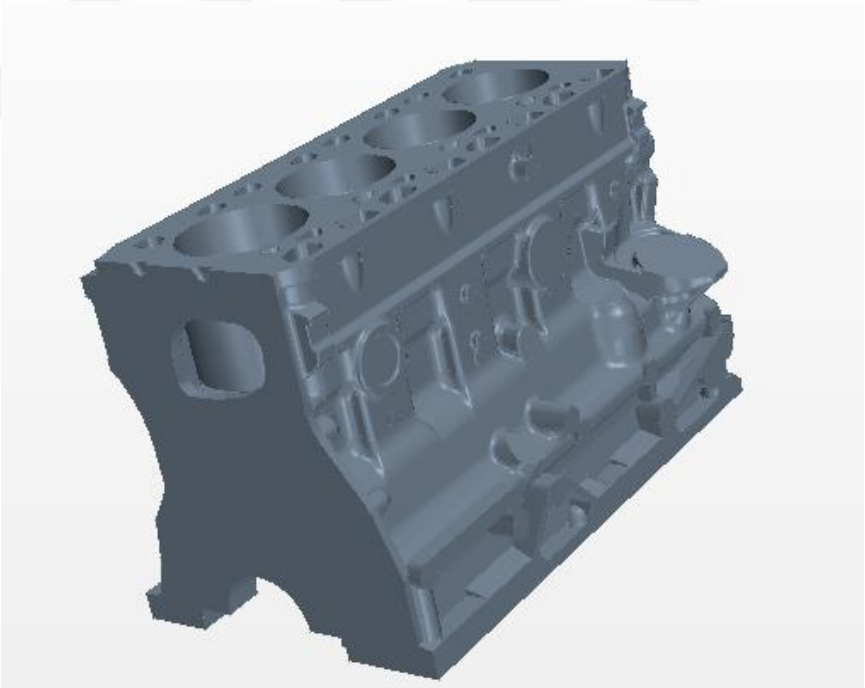

Figure 3.1: Base Engine Geometry of Engine Block

As seen from Figure 3.1, there are a number of ports, plugs, sharp geometries inside the block. To make an analysis all geometry is needed to be optimized to focus better analyzing of coolant. As shown in Figure 3.2, purple colored area is extracted from main body to create a flow area geometry to start the analysis.

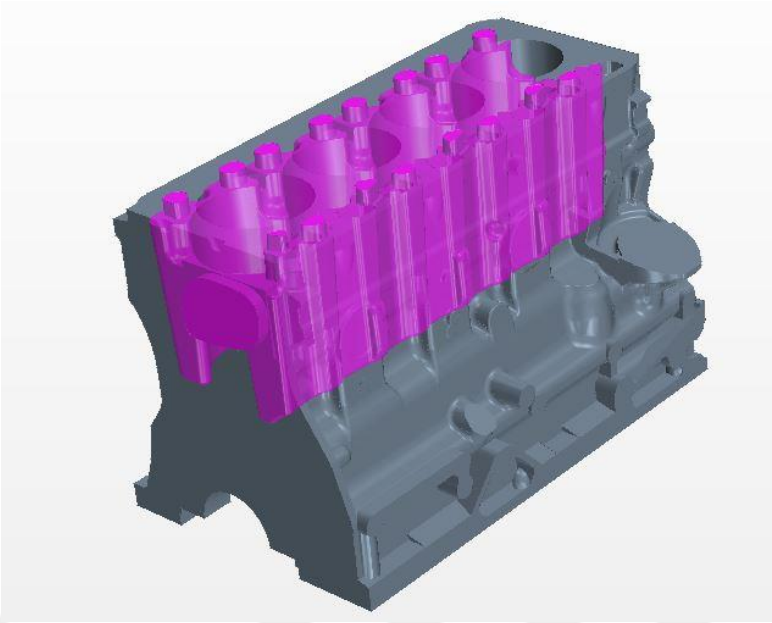

Figure 3.2: Extracted Water Jacket Volume in Diesel Engine Geometry

The analyzed geometry has a cold-water inlet section which is the red colored port. This vent directly works with pump pulley and water pump shown as in Figure 1.9 and 1.10. When the main engine is started, primary belt system also turns the pump pulley. This phenomenon starts water flow between heat exchanger and base engine block. In next sections, water flow rates and fluid properties are mentioned in detail.

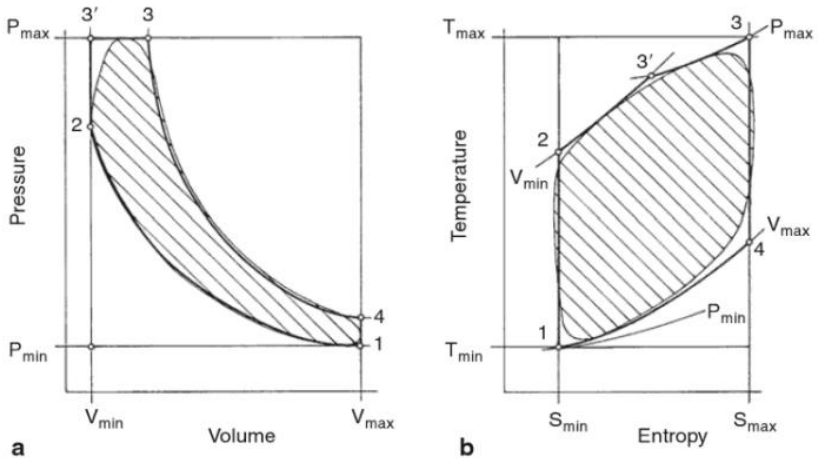

Figure 3.3: P-V and T-S Diagram for Industrial Diesel Engine [17]

In Figure 3.3, P-V and T-S graphs of a Diesel engine are shown. Maximum temperature is observed when maximum pressure occurs. [24]. For all steps due to combustion, heat transfer occurs and it causes the engine block temperature rise. This

raising should be controlled to maintain engine life, bushings, conrods and other systematic components' life. In this master thesis, after combustion, effected heat transfer will be simulated and calculated.

In Figure 1.6, the hot water outlet ports at the top of the block are in yellow colors. Eight pieces of vents are working to discharge hot water and to send it to a heat exchanger to be cooled.

3.2 ENGINE AND WATER PUMP SPECIFICATIONS

There are four main critical engine speeds. First, 1000 rpm which is called idle engine speed with no load condition. Second, 1400 rpm is the highest torque generated engine rpm as seen in Figure 3.4. Third, 1900 rpm is the highest power produced engine speed. Last, 2250 is the governed engine speed.

1900 rpm engine speed is the worst condition for heat generation, cylinder peak pressures, engine block volumetric stresses which are highest. Simulation studies are based on this condition. Torque, power and engine speed values are given in Table 2.1.

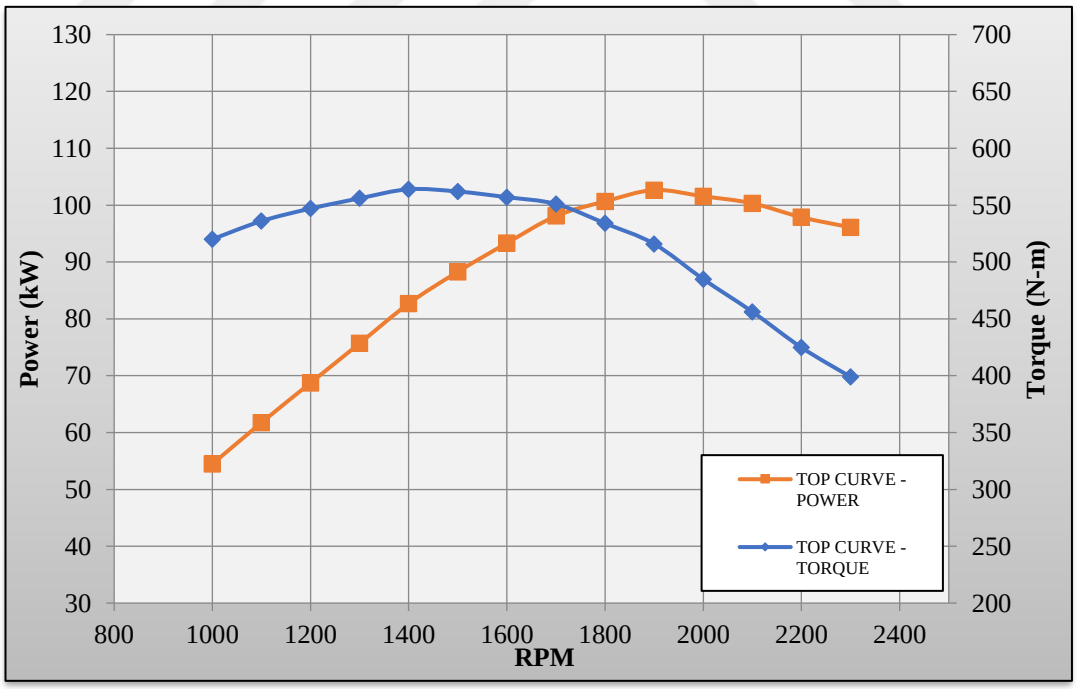

Figure 3.4: Engine Power-Torque-Speed Curve

Table 3.1: Engine Power Speed and Torque Chart

Engine Speed [rpm]	Crank Pulley Speed [rpm]	Engine Torque [Nm]	Engine Power [kW]
2550	2250	No Load Condition	No Load Condition
2500	2500	High Idler	High Idler
2450	2450	High Idler	High Idler
2300	2300	399	96
2200	2200	425	98
2100	2100	456	100
2000	2000	485	102
1900	1900	516	103
1800	1800	534	101
1700	1700	551	98
1600	1600	557	93
1500	1500	562	88
1400	1400	564	83
1300	1300	556	76
1200	1200	547	69
1000	1000	536	62
900	900	520	54
800	800	-	-

As seen in Table 3.1, 103 kW engine power is produced at 1900 rpm, which is called the maximum power produced stage. 546 Nm engine torque is produced at 1400 rpm, called the maximum torque produced stage. 2300 rpm and 800 rpm governed and idle speeds as mentioned in the previous sections. These specifications are directly belong to base engine geometry will be simulated in this study.

Water pump specifications can be seen in Figure 2.5 for five different speeds each creating a different flow rate and pressure on the system. Flow specifications directly change with engine speed. The ratio between engine speed and water pump pulley is 1.60.

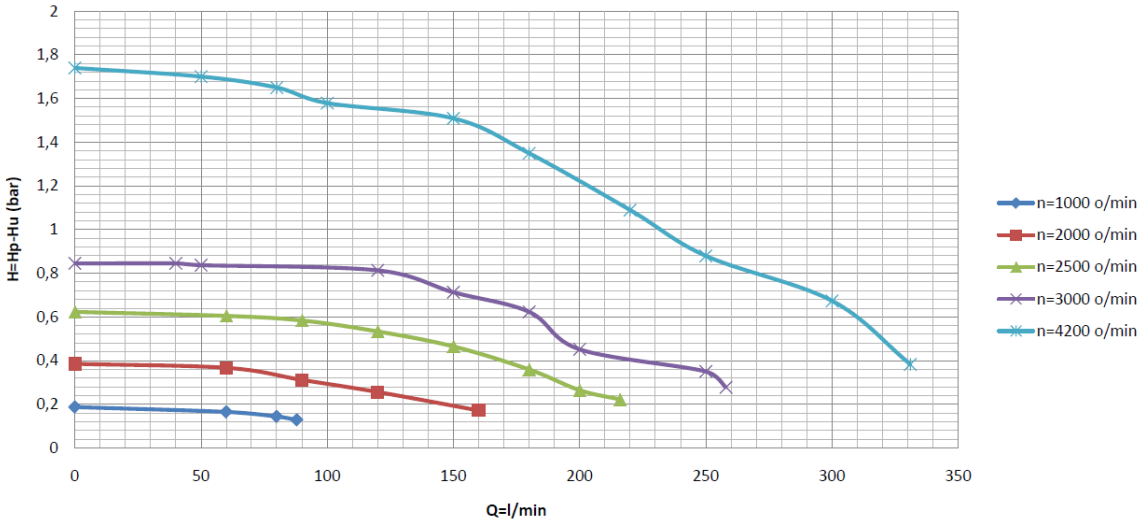

Figure 3.5: Water Pump Pressure[bar] versus Flow Rate[l/min]

3.3 WATER INLET SPECIFICATIONS

In Figure 3.6, the front face of the engine block is shown. Flow rate chart is used to calculate the water flow rate with respect to engine rpm. The water flow rate is one of the significant boundary conditions used in the analysis. The area of the water inlet section is calculated from 3D geometry.

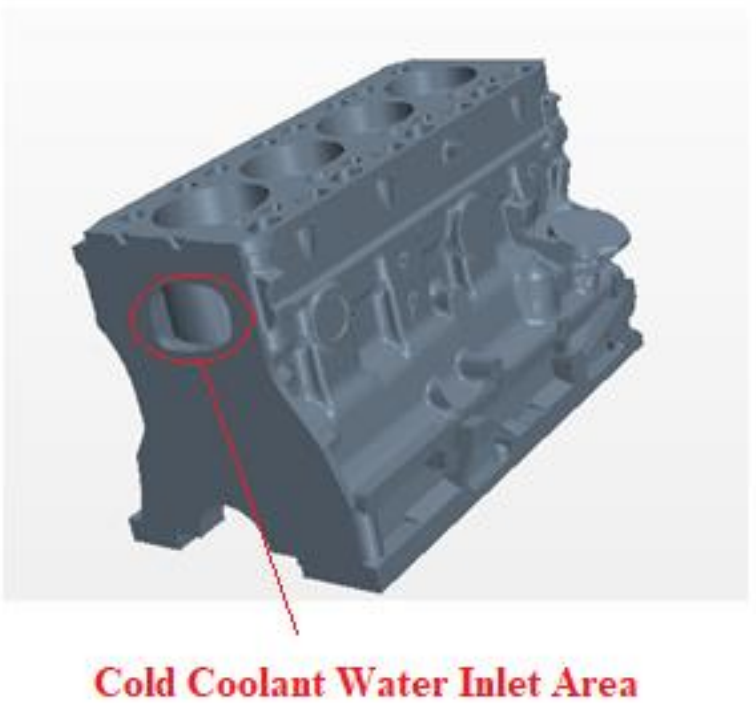

Figure 3.6: Cold Coolant Water Inlet Area

Fluid specifications are shown in below tables.

Table 3.2: Flow Coolant Speed with Different Engine and Water Pump Speeds

Rated Power Speed [rpm]	2300	1900	1400
Area of the Water Intake [mm^2]	5373		
Flow Rate [$^{l}/_{m}$]	250	170,86	80
Mass Flow Rate [$^{kg}/_{s}$]	4,2	2,87	1,34
Water Pump Speed [rpm]	3688	3207	2245
Flow Velocity [m/s]	0,77	0,53	0,24

Flow rates are calculated from the chart in Figure 3.5. Water pump speeds is calculated from the speed ratio of pulley which is mentioned in previous sections.

In this work, %50 water and %50 ethylene glycol mixture as the heat transfer fluid is used. In Table 3.3, the specifications of the fluid are shown.

Table 3.3: Coolant Mixture Properties at 50°C *[25]*

Fluid Density $[kg/m^3]$	1008.83
Specific Heat $[J/kgK]$	3582
Thermal Conductivity $[W/mK]$	0.39

3.4 SIMULATED GEOMETRY AND MESHING

As mentioned in Section 3, water jacket geometry is extracted from main body which is called flow area to be simulated. Meshed geometry is shown in Figure 3.6. Polyhedral mesh and surface remesher optimizer are used. For sharp edges aligned and curvature meshes are defined. Triangle meshing type are used due to complex geometry. 40.0 mm base size is used.

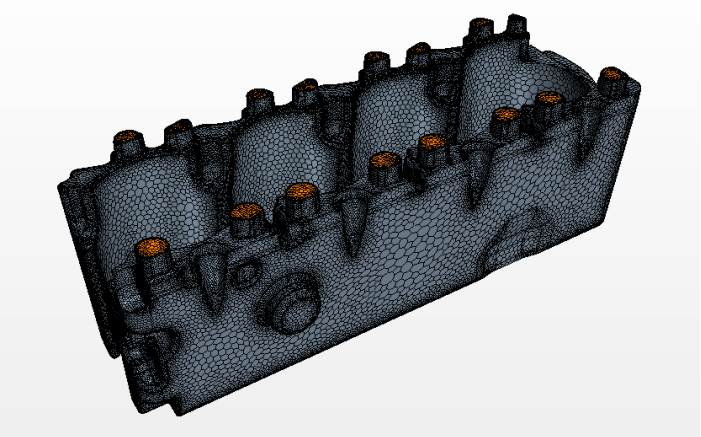

Figure 3.6: Meshing Structure of Water Jacket Flow Area

Surface curvatures circle size is 36.0. Curvature deviation distance is 0.01m. Proximity of points in gap is 2.0. Surface growth rate is 1.3. Volume growth rate is 1.2. Maximum cell size is directly arranged according to relative to base and 10000.0 percentage of base. Absolute size is 0.5m. Core mesh optimization threshold value is 0.4, optimization cycles are 1.

Figure 3.7: Most Critical Points During Meshing of Water Jacket Block

Most critical points during meshing of water jacket block are shown in Figure 3.7, as it can be seen from the figures, sharp edges of water inlet area and intersection of cylinder blocks are to be meshed in high quality to reach convergence. Nine different mesh size are tried to confirm mesh independence of the study. For each iteration, residual graphs are checked. 24722 mesh size are selected for entire study because residuals tend to reach 10^{-5}.

Table 3.4: Mesh Independency Study

Iteration	Number of Mesh Size	Average Temperature of Outlet, C
1	475595	97.5

Table 3.4 Cont.: Mesh Independency Study

Iteration	Number of Mesh Size	Average Temperature of Outlet, C
2	261233	97.5
3	191947	97.6
4	101498	97.4
5	73842	97.2
6	56132	97.6
7	34341	97.8
8	24722	97.1
9	10522	97.6

3.5 PHYSIC OF SOLVING MODELS

As it is mentioned in assumption section of study, constant density physics model is used for solution of the problem. Venkata Krishnan limited method based; accuracy level selector is 2.0. Cell skewness criterion, Chevron-cell creation assumptions are made. Least squares tensor minimum eigenvalues ratio 0.1. Normalized flat cells curvature factor 1.0. Maximum safe skewness angle is 75°. Minimum unsafe skewness angle is 88°. 2^{nd} order convection segregated properties are used. Positivity rate limit is 0.2.

During the simulation, reference values of fluid physics for initial run is shown in Table 3.5.

Table 3.5: Reference Values of Fluid Physics

Maximum Allowable Absolute Pressure [Pa]	$1.0e^{8}$	Static Temperature[K]	300
Minimum Allowable Temperature[K]	100	Velocity[m/s]	0
Minimum Allowable Absolute Temperature [Pa]	1000	Reference Pressure [Pa]	101325.0
Maximum Allowable Temperature[K]	5000	Coordinate System	Laboratory

3.6 ASSUMPTIONS

The CFD simulation is done by Star CCM+. The main assumptions and considerations about the simulation can be regarded as:

- Steady state condition is assumed for the entire analysis.
- For the entire fluid analysis constant density for %50 water-%50 ethylene glycol fluid properties are used. Specifications are listed in Table 11.
- Three-dimensional flow is assumed.
- k- ε turbulence solver is used for entire study.
- Reynolds-Averaged Navier Stokes equations are used for entire study.
- Segregated flow temperature and temperature gradients solving method are used.
- Upper block geometry details are ignored.
- Engine vibrations, adessive shocks, ambient temperature of climate conditions are ignored.
- Contamination effects are ignored.
- Manufacture faults, pump quality characteristic, assembly faults are ignored.
- Firing order is ignored. All CFD simulations will be implement as all cylinders are firing at same time without any sequences.
- 210°C is going to take into essential for constant cylinder wall temperatures.
- Heat transfer coefficient is not correlated with Crank Angle [CA].

3.7 BOUNDARY CONDITIONS

For the studies, fist verification with actual test result is done and regarding these simulations, boundary conditions used when the engine speed is 1900 rpm can be seen below.

For water inlet section,

Table 3.6: Inlet Fluid Boundary Conditions

Flow Direction Specification	Boundary Normal
Reference Frame Specification	Lab Frame
Turbulence Specification	Intensity + Viscosity Ratio
Velocity Specification	Magnitude + Direction
Static Temperature, °C	96.0
Turbulence Intensity	0.01, Constant
Turbulence Viscosity Ratio, Constant	10
Velocity [m/s]	0,53

For water outlet section,

Table 3.7: Outlet Fluid Boundary Conditions

Backflow Specification	Boundary-Normal
Pressure Outlet Option	None
Reference Frame Specification	Lab Frame
Turbulence Specification	Intensity + Viscosity Rati
Static Temperature of Ambient, °C	110.0
Pressure, Pa	1.6
Turbulence Intensity	0.01, Constant
Turbulence Viscosity Ratio, Constant	10

CHAPTER IV
VALIDATION STUDY AND EXPERIMENTAL VERIFICATION OF THE MODEL

4.1 EXPERIMENTAL STUDY FOR VERIFICATION

Before further studies and simulations, to make sure the model is valid, CFD models and results should be compared to actual test results. To do this, realistic test bench is prepared, and realistic engine is mounted on this bench. To reach most critical cylinder peak pressures, engine is run at 1900 rpm and relevant measurements are done on the test bench.

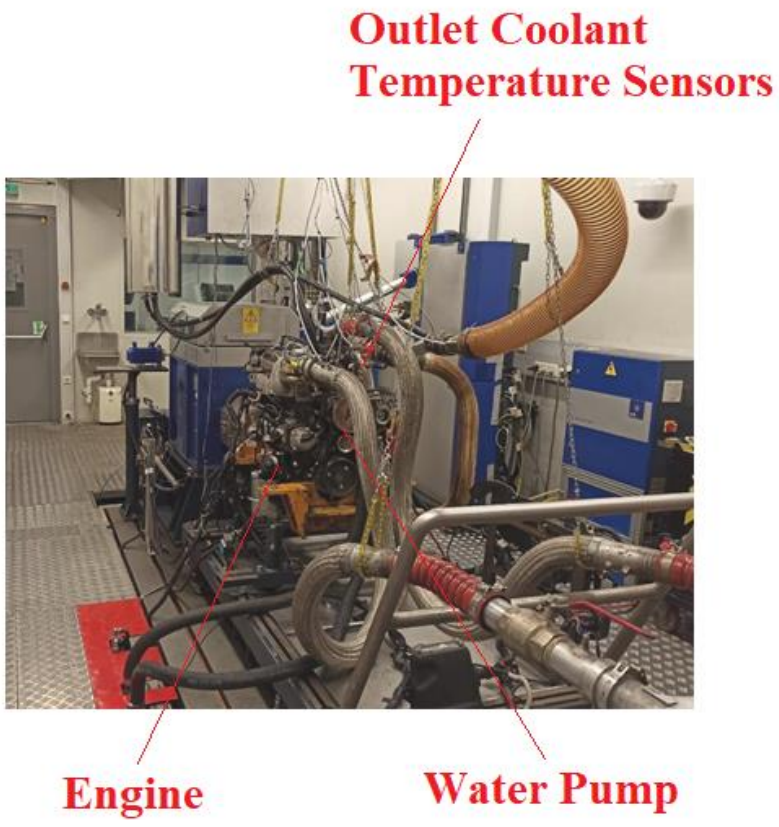

Figure 4.1: Test Bench to Measure Water Circuit Temperature of Engine Block

In Figure 4.1, test bench to measure inlet and outlet temperature values of coolant temperature can be seen. Radiator coolant pressures, engine speeds also measured.

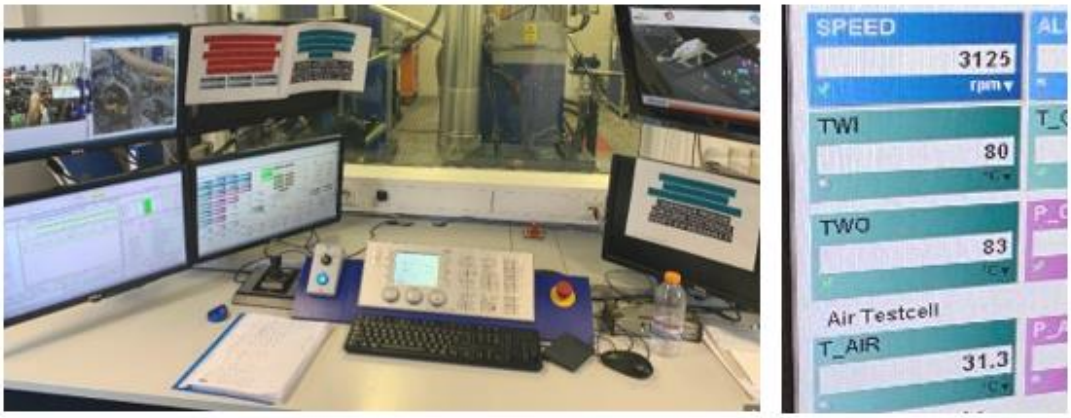

Figure 4.2: Test Bench Cockpit

As shown in Figure 4.2, all test data can be monitored and recorded in the test bench cockpit.

4.2 TEST BENCH RESULTS

Test bench activities are done to measure temperature values among the engine block for three different engine rpm, 1400,1900 and 2300 as mentioned in previous sections to ensure the test bench operates correctly and the values found are accurate. Values found for 1900 rpm are used to make the validation of the numerical model. During testing, radiator inlet and outlet temperatures, LAT, Intercooler inlet and outlet temperatures, intercooler inlet ant outlet pressures are recorded as seen in the Figure 4.3. On Table 4.1, radiator inlet and outlet temperature values can be seen which are compared with values found by numerical simulations. Also, test is made when engine is fully loaded, all accessories like climate compressor, alternator, air compressor are opened.

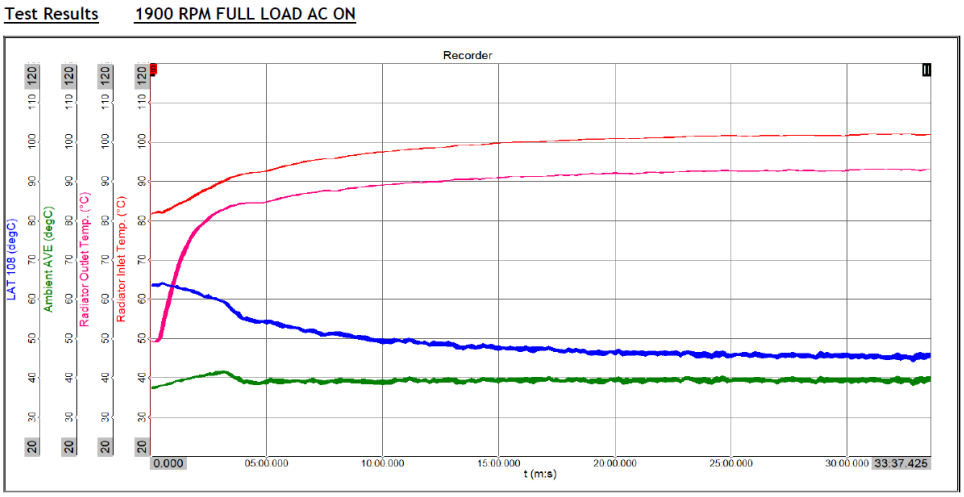

Figure 4.3: 1900[rpm] Engine Test Results

When the main engine speed is 1900 rpm, temperature values are plotted in Figure 4.3.

Table 4.1: Engine Temperature Chart During Maximum Power Speed

Radiator Inlet Temperature, °C	101.9	LAT, °C	45.4
Radiator Outlet Temperature, °C	93.0	Intercooler Inlet Temperature, °C	190.4
Ambient Temperature, °C	39.4	Intercooler Outlet Temperature, °C	74.5

4.3 NUMERICAL VALIDATION OF WATER JACKET

As mentioned in pervious sections, for all engine speeds boundary conditions and input values had been calculated. In previous section, realistic test bench results are measured by using engine test bench for four-cylinder applications.

As it can be seen from Table 4.1, radiator inlet temperatures which means engine water jacket temperatures are measured. Below simulation results are compared with CFD results for numerical validation of the study.

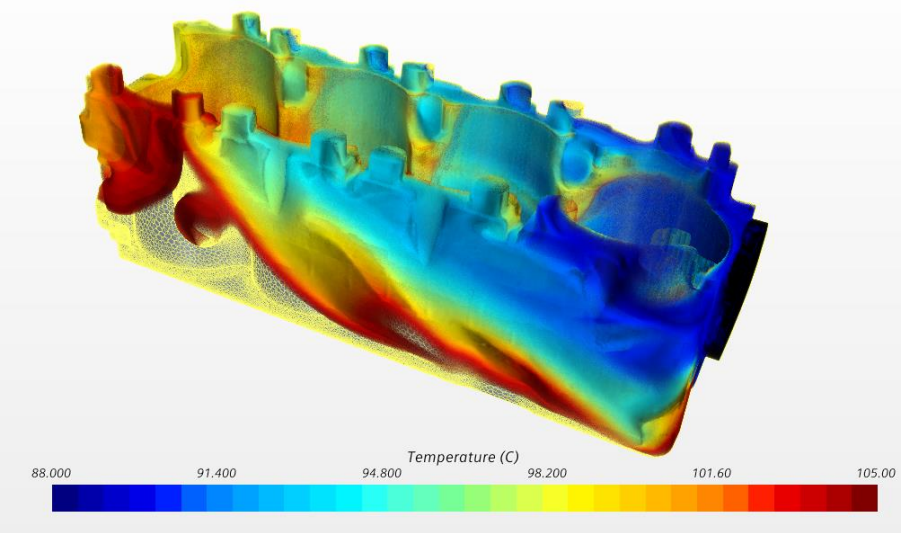

Figure 4.4: Temperature Distribution of Water Block After Combustion

As it can be seen from first run of study, when water enters from water inlet port of jacket, from first cylinder to last one, temperature increase is detected as normally due to geometrical design of passages and internal structures. As mentioned before in geometry preparation section of study, sixteen outlet port works to discharge pumped hot water from main body to send heat exchanger to be cooled. As it can be seen from the figure, all port temperature distributions are different from each outer as normally. 91-92°C is measured on first cylinder ports, on the hand 105-106°C water temperature is measured from last cylinder nearest ports. When water enters to water jacket, lower levels of temperature is higher than outlet section's ports except fourth cylinder. Lower temperature is set to 88-90°C because measured outlet temperature from the test bench activity is similar.

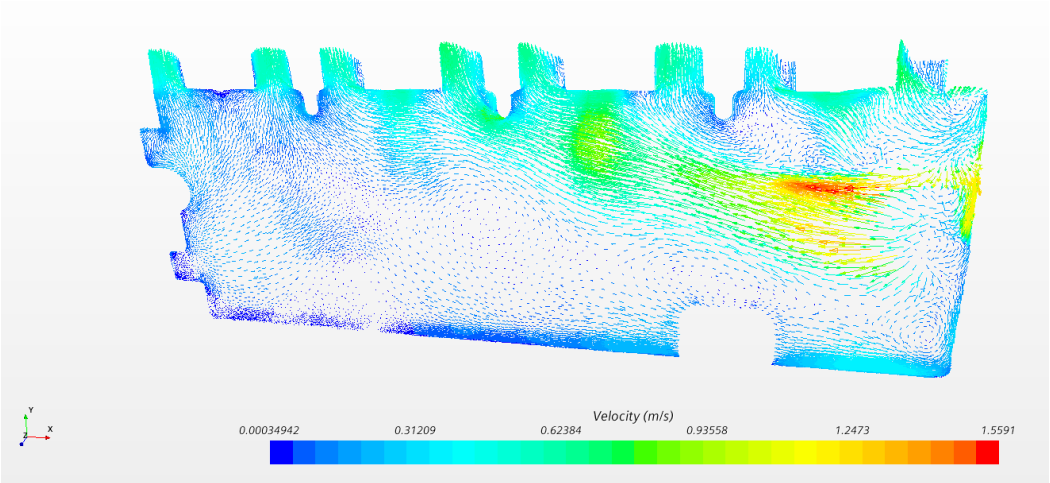

Figure 4.5: Velocity Distribution of Water Block After Combustion

Velocity distribution is shown in Figure 4.5, as mentioned before virtual validation is done. From figure, it can be seen that maximum velocity found as 1.5 6m/s. In water jacket, middle of block, 0.3-0.4 m/s flow temperature is calculated. 0.9-1.2 m/s flow velocity is calculated also on outlet ports.

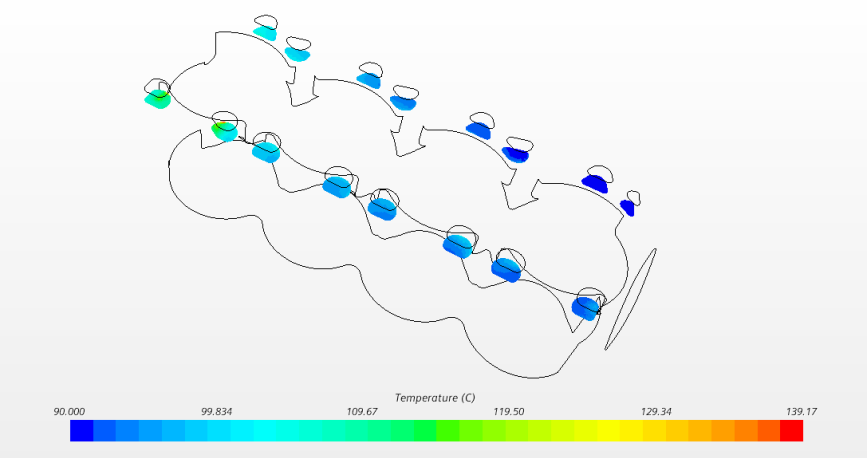

Figure 4.6: Cross Section of Ports and Temperature Distribution of Outlet Ports

As it can see from Figure 4.6, average temperature is calculated from Star CCM+, and the results show that 97.1°C coolant temperature is observed on outlet ports. Measured radiator inlet temperature is 101.9°C. Difference between measured and calculated value is 4.8°C. According to the results, error is 10 % and acceptable, and the geometrical model and boundary conditions can be accepted as valid to start the study of enhancement on block to reduce temperature. In Figure 4.8, HTC distribution of water jacket during combustion is shown. 2006 W/m^{2}K is analyzed.

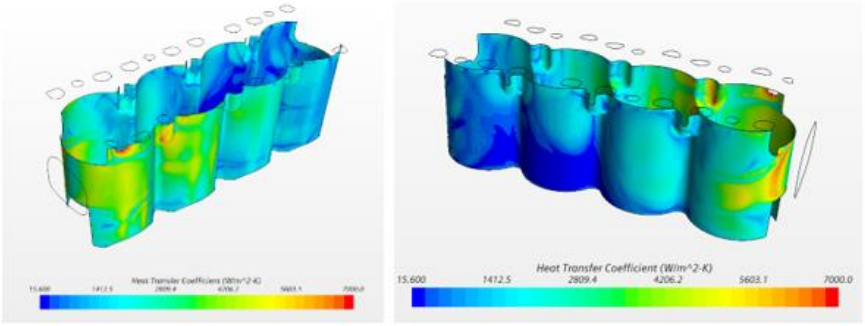

Figure 4.7: HTC Distribution of Water Jacket

CHAPTER V
NUMERICAL METHODOLOGY FOR HEAT TRANSFER ENHANCEMENT BY GEOMETRICAL MODIFICATION

The main aim of this study is enhancement of thermal performance of the engine block by geometrical modifications on engine block and decreasing the outlet temperature of the engine coolant. In Table 5.1, studied cases are shown.

Table 5.1: Cases for Geometrical Modification

Simulated cases	Description	Number of outlet ports	Shape of ports
Case 1-Base Case	Validation case	16	Elliptic, Semilunar
Case2	First geometrical modification	23	Elliptic, Semilunar, Hole
Case3	Second geometrical modification	8	Slot
Case4	Third geometrical modification	2	Linked Slot

Case 1-Base Case is used for actual model validation described in Chapter 4. Case 2, Case 3 and Case 4 are the new models which are simulated and presented in the following sections. Water inlet sections, cylinder bore diameters and internal channels are not changed during modifications. All the assumptions listed in Chapter 3 are valid for these new simulations as well as the inlet and outlet boundary conditions, wall temperatures given in Table 3.6 and 3.7. In the following part, optimized geometries of outlet ports of the engine block can be seen regarding case numbers.

5.1 CASE 1-BASE CASE SIMULATIONS

This case is also called the validation case in this study which is already described in Chapter 4. As it can be seen in Figure 4.6, average coolant temperature is calculated as 97.1°C on outlet ports. In Figure 4.8, case 1 HTC results are shown. 2006 W/m^2K HTC is analyzed.

In Figure 5.1, Case 1 geometry is shown. The actual outlet port design is also shown with red circles.

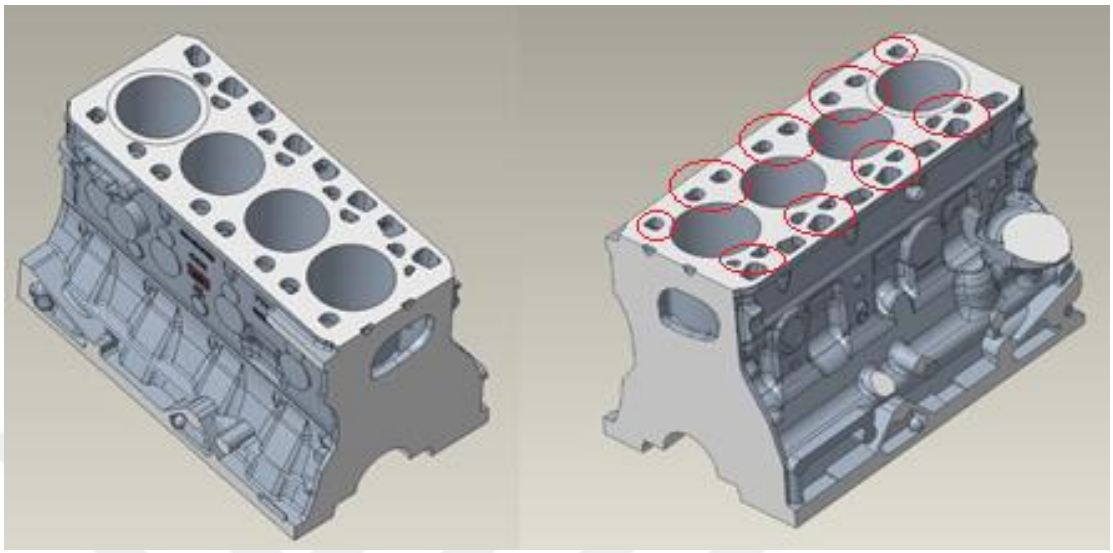

Figure 5.1: Case 1-Base Case CAD Geometry

5.2 CASE 2 SIMULATIONS

The first optimized geometry is shown in Figure 5.2. Added ports are shown with red circles. 12 mm seven holes are added to outlet ports to reduce the average temperature distribution of the block. Internal pressures are directly affecting the resistance of water in the jacket. This case aims to reduce flow resistance and pressure on outlet ports.

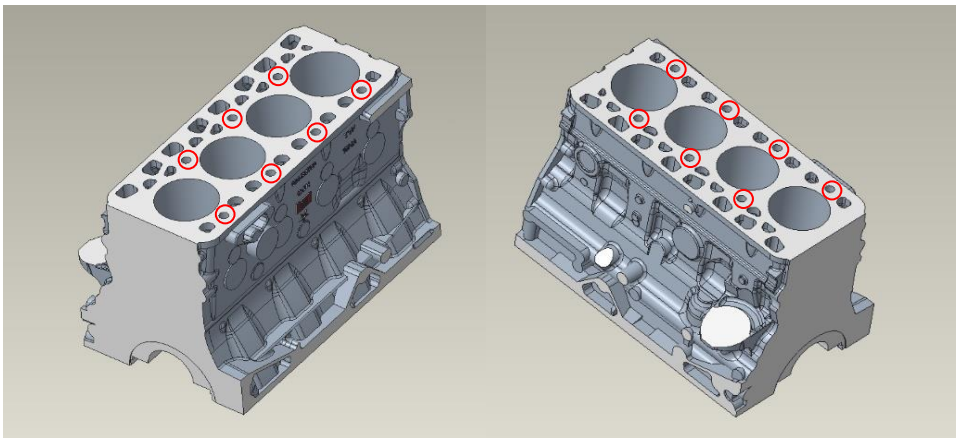

Figure 5.2: Case 2 CAD Geometry

In Figure 5.3, Case 2 simulation is shown. 95.6°C averaged temperature is analyzed on the outlet ports. Outlet temperature for this case is shown to decrease %0.5 with respect to validated Case 1.

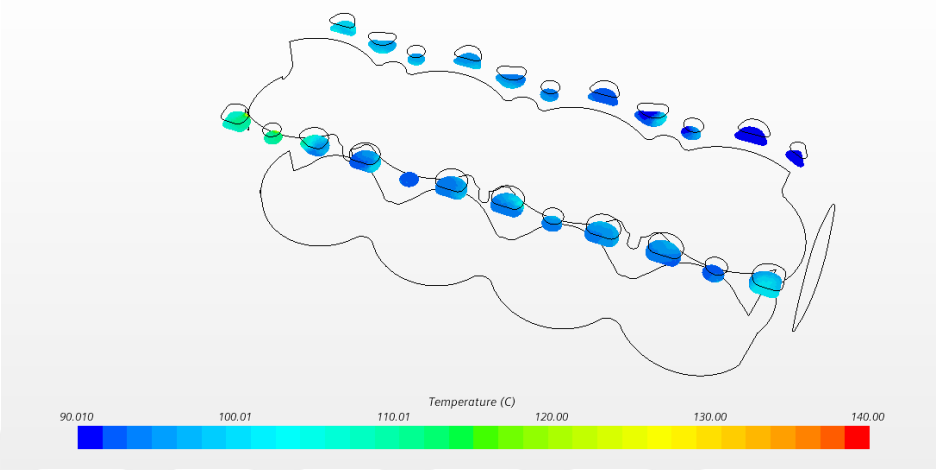

Figure 5.3: Case 2 Temperature Distribution

In Figure 5.4, heat transfer coefficients for Case 2 can be seen on the engine block geometry. The surface average heat transfer coefficient is found as 1733 W/m^{2}K. Distribution of similarity is observed with Case 1. When compared to Case 1, HTC is shown to decrease %7.

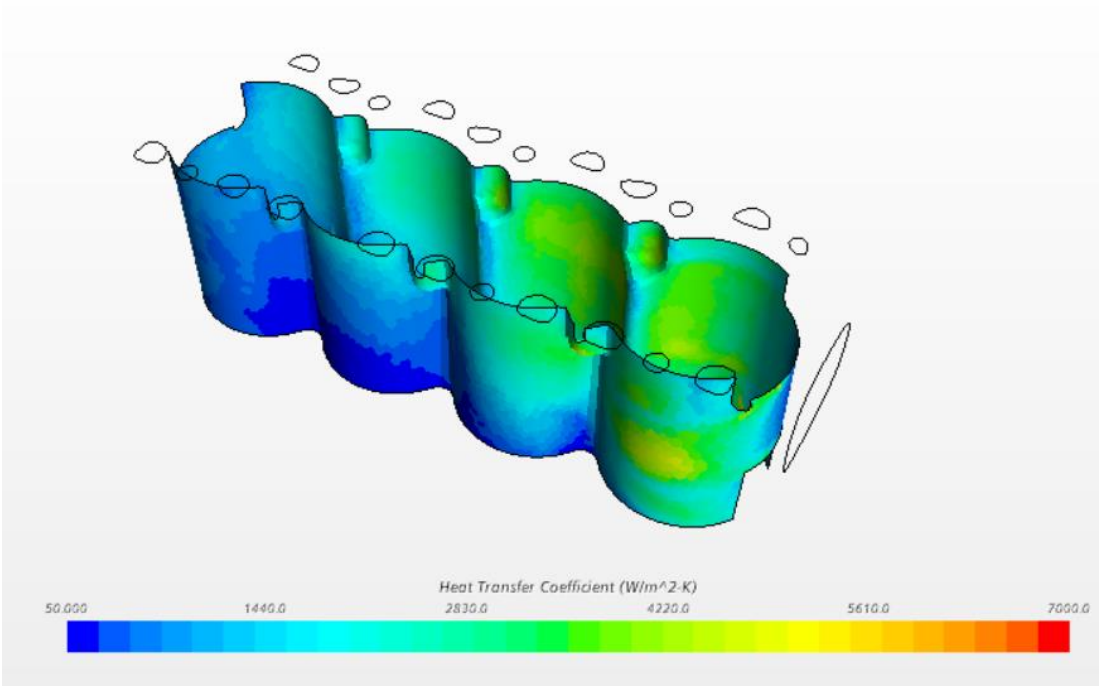

Figure 5.4: Case 2 Local HTC Distribution

5.3 CASE 3 SIMULATIONS

In Figure 5.5, the second simulated case is shown. All actual holes are canceled, eight pieces of slots are added to geometry as outlet ports. A lot of commercial engine manufacturers are researched during the study. This slotted form is inspired by VW 1.4 Golf TSİ. In Figure 5.6, Case 3 simulation is shown. 95.7°C averaged temperature is analyzed on the outlet ports.

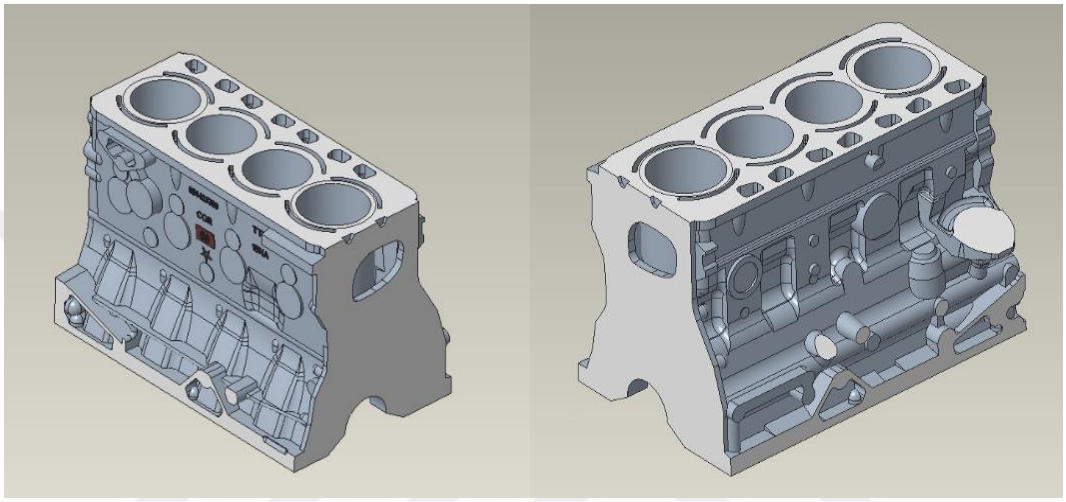

Figure 5.5: Case 3 CAD Geometry

Outlet temperature for this case is shown to decrease %1.5 with respect to validated Case 1.

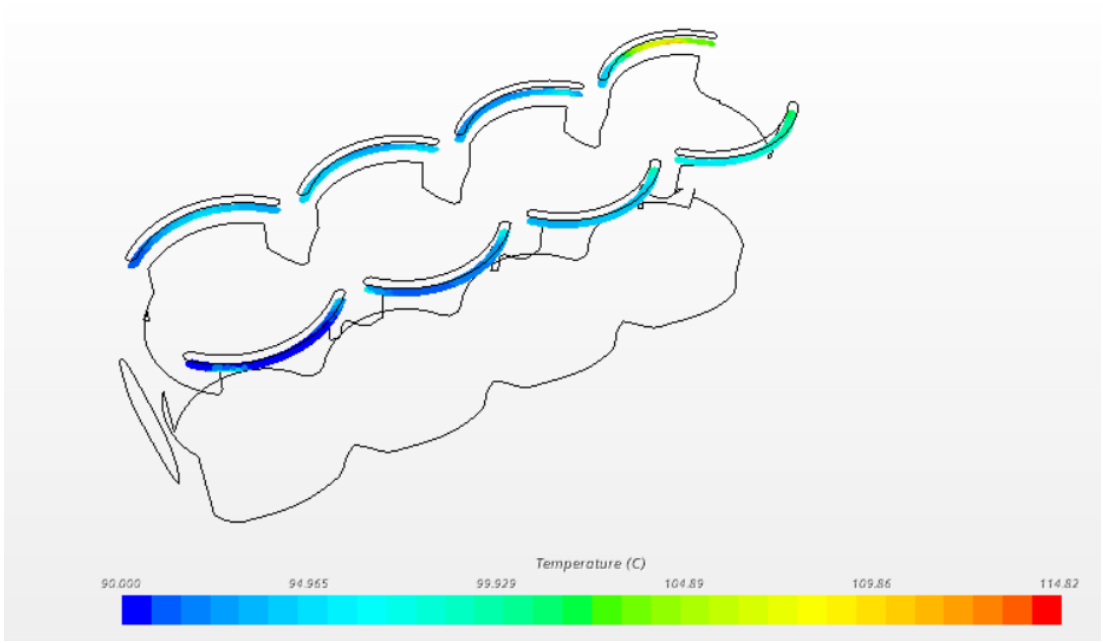

Figure 5.6: Case 3 Temperature Distribution

In Figure 5.7, Case 3 local Heat Transfer Coefficient simulation results are shown. 1580 W/m^{2}K for surface average heat transfer coefficient are analyzed on volume mesh. Distribution of similarity is observed between with case 1 and 2. When compared to Case 1, HTC is shown to decrease %5.43.

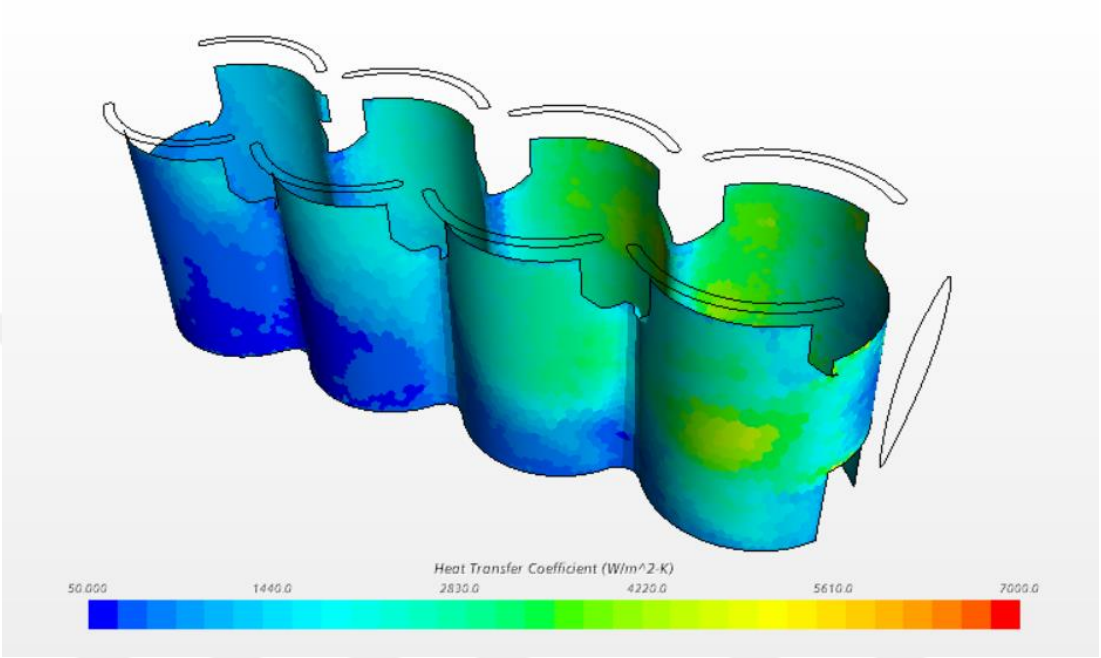

Figure 5.7: Case 3 HTC Distribution

5.3. CASE 4 SIMULATIONS

In Figure 5.8, third and last simulated Case 4 is shown. All slots are linked to each other, totally there are two different outlet ports on left and right side of block. This form is inspired by both Renault and VW engines.

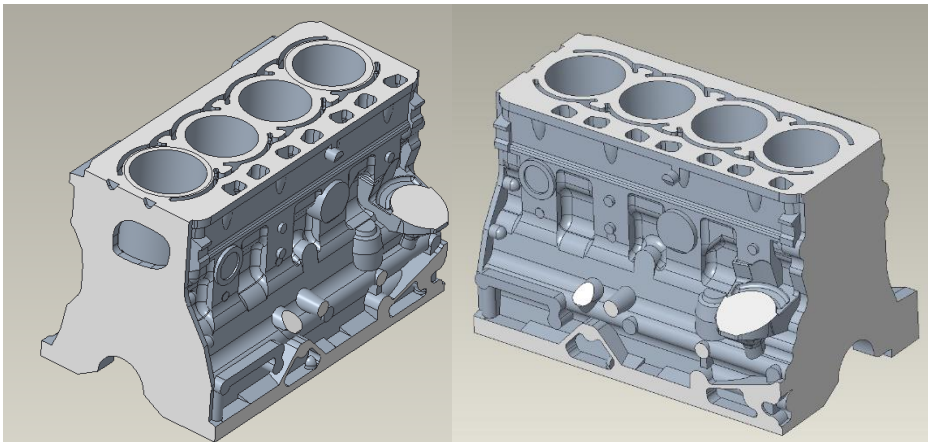

Figure 5.8: Case 4 CAD Geometry

In Figure 5.9, Case 4 temperature distribution simulation is shown. 91.1°C averaged temperature is analyzed. 6°C outlet port temperature difference is analyzed between Case 1 and Case 4. Outlet temperature for this case is shown to decrease %6 with respect to validated Case 1.

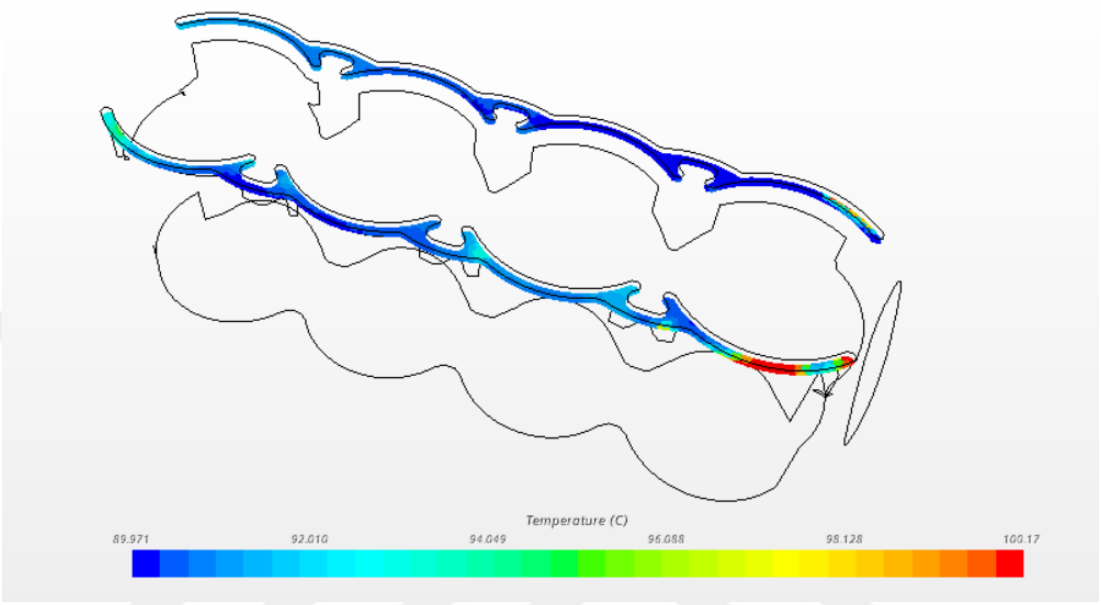

Figure 5.9: Case 4 Temperature Distribution

Case 4 is determined to be the most efficient case regarding both the temperature values and HTC values. Further analysis is done for Case 4 given below. Maximum temperature is observed on forth cylinder left side of slot. In Figure 5.10, temperature distribution of this cylinder is shown. 99-100°C port temperature is analyzed on the first cylinder left side of outlet port.

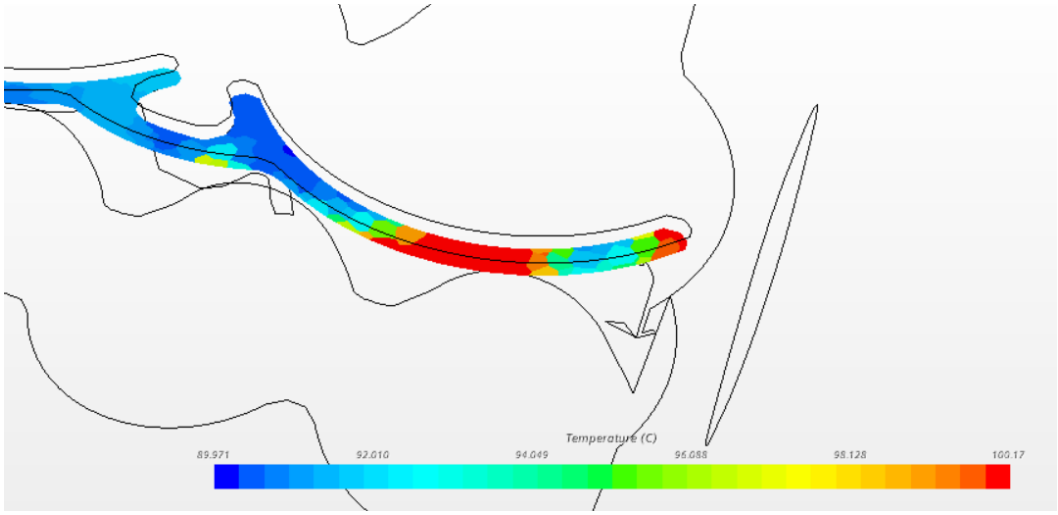

Figure 5.10: Maximum Temperature Points on Case 4

In Figure 5.11, Case 4 HTC results are shown. 196 W/m^{2}K for surface average heat transfer coefficient are analyzed on volume mesh. Case 4 has the lowest and best HTC value among studied cases. Homogenous distribution and most critical values are observed on intersection points between cylinders.

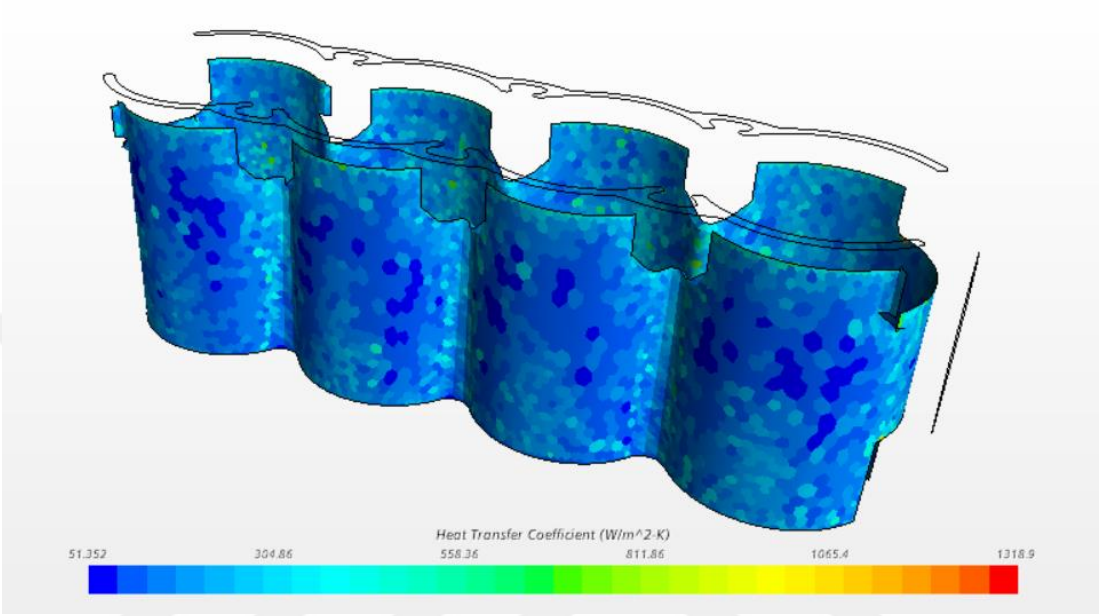

Figure 5.11: Case 4 HTC-Scaled Distribution

CHAPTER VI
RESULTS AND DISCUSSION

For the study, a numerical investigation is carried out to geometrically modify the base engine water jacket geometry for enhancement of heat transfer from the engine block.

Base geometrical model which is prepared by using Star CCM + with appropriate boundary conditions is validated by testing the real engine in laboratory conditions. Geometry enhancement and optimization of CFD studies are also performed by using Star CCM + and the results of the simulations for designed new outlet port geometries regarding three different cases are given in the previous chapter. Below, a summary result table can be seen regarding temperature enhancement for each proposed model for Case 2, 3 and 4.

Table 6.1: Average Temperature of Outlet Ports

Geometry	Average Temperature of Outlet Port, °C	Enhancement Percentage %
Case 1-Base Case	97.1	-
Case 2	95.6	0.5
Case 3	95.7	1
Case 4	91.1	6.1

In Table 6.1, average temperature results of the outlet port are listed for each designed outlet port geometry and simulated case. Enhancement Percentages of Case 2 and 3 are so close to case 1. On the other hand, considering case 4 results, it is observed that there is a significant improvement compared to the base model. 6.1% coolant temperature improvement is found to have a significant importance in terms of engine performance and life for CI engines.

In Figure 6.1, Case 4 middle section temperature distribution is shown. Linked geometry reduced each cylinder outlet port temperature. No abnormal temperature values are observed.

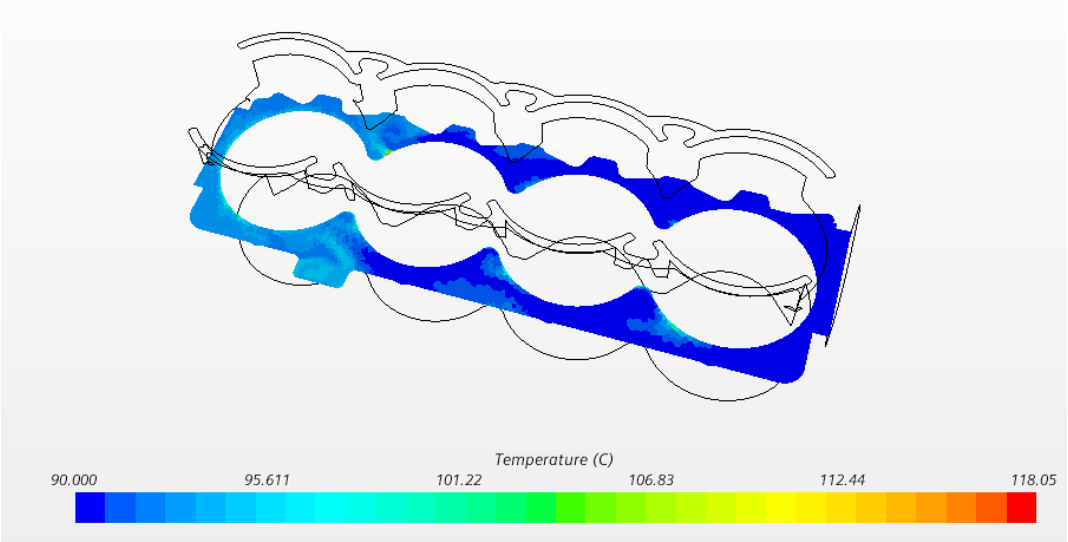

Figure 6.1: Case 4 Middle Section Temperature Distribution

It is very important to investigate engine block geometry to analyze left and right port sections internal temperature behavior. In Figure 6.2, right section temperature distribution is shown. No abnormal behavior is observed. The temperature increase on fourth cylinder block is considered as normal and there is no back flow observed.

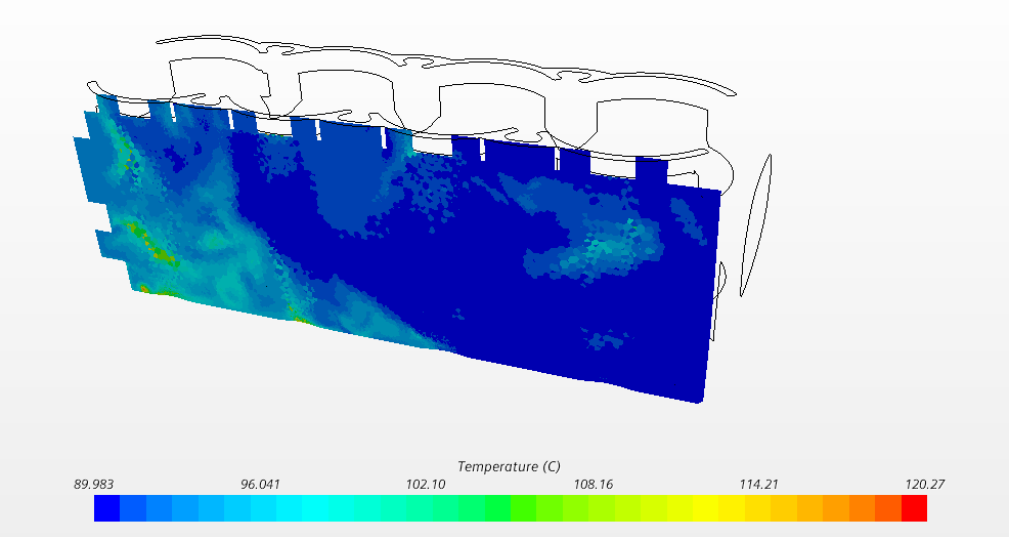

Figure 6.2: Case 4 Right Section Temperature Distribution

In Table 6.2 average heat transfer coefficient distribution for each case is shown. No abnormal behavior is observed. Case 1, 2 and 3 simulation results are quite similar, but acceptable. Case 4 HTC value is found to be significantly low compared to Case 1, which is the base case.

Table 6.2: Average HTC Distribution of Iterations

Geometry	Average HTC Distribution, W/m^2K
Case 1	2006
Case 2	1733
Case 3	1580
Case 4	202

For CI Engines, average heat transfer coefficient increase is essential between the cylinder layer and the water jacket. According to the literature, HTC distributions for CI engines are a function of the number of cylinders, maximum governed speed and volume of engine. From 150 to 11500 W/m^2K HTC values take place in literature for similar CI engines. For Case 4, 202 W/m^2K HTC distribution value is acceptable according to the literature results. [26] [12] [27]

As a summary; three different cases regarding different designed outlet port geometries have been simulated and results of the simulations are compared with the base engine CFD model which has been validated by experiments. Regarding the findings, below results can be summarized for the study:

- All cases show some level of improvement regarding the temperature values and heat transfer coefficient values inside the engine block.
- Case 4 is the best case compared to Case 1 and other two cases regarding overall performance.
- %6.17 coolant temperature enhancement is achieved in Case 4 compared to Base case.
- Volumetric flow rate of the coolant is 0.53 lt/s.

Recommendations for future work,

- Manufacturability analysis must be made due to changing geometry on ports.
- Upper block design geometry must be checked due to changing geometry.
- Detailed validation operation must be performed on physical engine to eliminate any possible risk on block.

REFERENCES

[1] R. Basshuysen, "Introduction," in *IC Engines*, 7 West Patel Nagar, Tata McGraw Hill Education Private Limited, Fourth Edition, 2012, p. 60.

[2] C. Frank, "Ford Model An Album," *Polyprints*, p. 49, 1960.

[3] W. Pulkrabek, "Introduction," in *Engineering Fundamentals of Internal Combustion Engines*, Platteville, Pretice Hall Upper Saddle River, New Jersey 07458, 2016, pp. 1-2.

[4] O. Volpato, "Control System for Diesel - Compressed Natural Gas Engines," Conference: 14º SIMEA - Simpósio Internacional de Engenharia AutomotivaAt: São Paulo, SP. Brazil.

[5] M. Antonio, "Design and Analysis of a Cooling Control System of a Diesel Engine to Reduce Emission and Fuel Consumption," *ABCM Symposioum Series in Mechatronics Vol 5*, vol. 5, no. Section II, p. 39, 2012.

[6] J.Walker, "The GM 1.8 Liter Gasoline Engine Designed by Chevrolet,," *SAE paper 820111*, p. 397, 1982.

[7] R. Goud, "Design and Thermal Analysis of Cylinder Block," *International Journal of Advance Research in Science and Engineering*, vol. No 6, no. 01, p. 25, 2017.

[8] R. Yeswanth, "Design of Optimization of Engine Blcok," *IRE Journal*, vol. 5, no. 1, pp. 6-16, July 2021.

[9] R. Stone, "Introduction," in *Introduction to Internal Combustion Engines*, Uxbridge, Middlesex, Brunel Unibersity, Machillan, 1192, pp. 10-20.

[10] W. Pulkrabed, "Chap 10. Heat Tranfer in Engines," in *Engineering Fundamentals of the Internal Combustion Engine*, pp. 339-345.

[11] J. Liljedalh, "Engine Accessories," in *Tractors and Their Power Units*, New York, Wiley, 1979, pp. 156-181.

[12] Z. Ping, "Computational Fluid Dynamics Tehnology Applied in Flow Analysis in Diesel Engine's Cooling Water Jacket," *Second International Conference on Intelligent Human-Machine Systems and Cybernetic,* pp. 1-3, 2010.

[13] Y. Zhang, "Optimization Design for Water Jacket of 4G24 Gasoline Engine," *IEE*, pp. 1-4, 2011.

[14] O. Guangyao, "Study on Solid-Fluid Coupled Heat Transfer Simulation of Cylinder Head of High Power Density Diesel Engine," *International Conference on Intelligent Computation Technology and Automation,* pp. 1-3, 2010.

[15] G. Subbarao, "Optimization of Water Jacket Using CFD for Effective Cooling of Water-Cooled Diesel Engines," *SAE-2007-26-049,* vol. 049, pp. 567-576, 2007.

[16] D. Peng, "Study on Solid-Fluid Coupled Heat Transfer Simulation of Cylinder Head of High Power Density Diesel Engine," *International Conference on Intelligent Computation Technology and Automation,* vol. 1, no. 1, pp. 1-3, 2010.

[17] A. Paratwar, "Surface Temperature Prediction and Thermal Analysis of Cylinder Head in Diesel Engine," *International Journal of Engineering Research and Applications(IJERA),* vol. 3, no. 4, pp. 892-902, 2013.

[18] O. H. Robert Armstrong, Dynamics of Polymeric Fluids: Fluid Mechanics 1, NY: Wiley-Volume 1, 1987.

[19] B. Bird, "Generalization of Newton's Law of Momentum," in *Transport Phenomena*, NY, 2nd Edition, Wiley, 2002, pp. 11-37.

[20] J. Anderson, "Governing Equations of Fluid Dynamics," in *Wendt, J.F. (eds) Computational Fluid Dynamics.*, Berlin, Heidelberg, 1992, p. 20.

[21] B. Launder, "The Numerical Computation of Turbulent Flows," in *Computational Methods in Applied Mechanics and Engineering*, 1974, pp. 269-289.

[22] B. Launder, "Application of the Energy Dissipation Model of Turbulence to the Calculation of Flow Near a Spinning Disc," in *Letters in Heat and Mass Transfer*, 1974, pp. 131-138.

[23] W. Kays, Convective Heat and Mass Transfer, McGraw Hill Inc., 1993.

[24] K. Tschoeke, "Handbook of Diesel Engines," Berlin Germany, Springer, pp. 265-269.

[25] G. Sekrani, "Thermophysical Properties of Water Ethylene Glycol Mixture Based Review on Their Thermophysical Properties," *Applied Science,* p. 9 of 23, 2018.

[26] M. Chamani, "Numerical Investigation of Heat Transfers In the Water Jacket of Heavy Duty Diesel Engine by Considering Boiling Phenomenon," *Elseiver, Case Studies in Thermal Engneering 12 (2018) 497-509,* pp. 502-Table 2, 2018.

[27] S. Sivan, "Enhancement of Heat Transfer of Cylinder Liner and Coolant Jacket for High Powered Diesel Engine," *Elseiver, Science Direct,* p. 1493, 2020.

[28] Marcel Davis, "Study of Heat Transfer Analysis of Diesel Engine Head," *Acta Polytechnica,* vol. 43, p. 5/2003, 2001.

[29] H. Bilginberk, "Güç ve Verim Dizel Motorları," Istanbul, Etüd ve Programlama Dairesi Yayınları, 19780, pp. 33-46.